2025/04/15 @ “Lepton flavor change in nuclei”, ECT*, Trento

Calculations of various muon decays in orbit

Contents

1. Introduction (2 slides)
2. Calculating lepton wave functions (7 slides)
3. Decay in orbit (10 slides)
4. μ-e conversion (8 slides)
5. Other lepton flavor violating processes
   - 5-1. $\mu^- \to e^- X$ (8 slides)
   - 5-2. $\mu^- \to e^- \gamma$ (7 slides)
   - 5-3. $\mu^- e^- \to e^- e^-$ (8 slides)
6. Summary

Yuichi UESAKA

Dokkyo Medical University

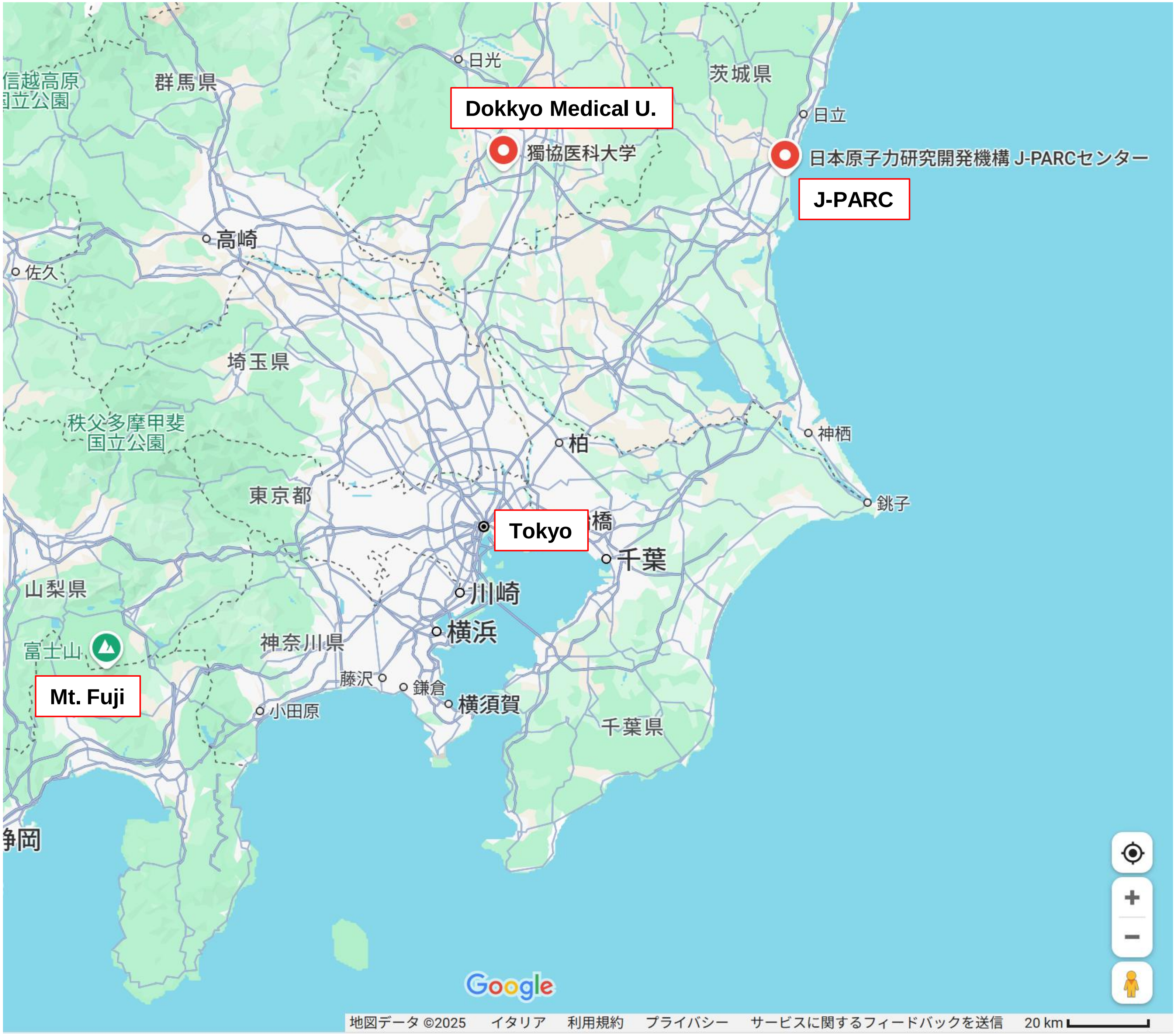

Dokkyo Medical U.
獨協医科大学
日本原子力研究開発機構 J-PARCセンター
J-PARC
Tokyo
Mt. Fuji
富士山
日光
日立
茨城県
群馬県
信越高原
国立公園
高崎
佐久
埼玉県
秩父多摩甲斐
国立公園
柏
神栖
銚子
東京都
千葉
川崎
横浜
山梨県
神奈川県
藤沢
鎌倉
横須賀
小田原
千葉県
静岡
地図データ ©2025 イタリア 利用規約 プライバシー サービスに関するフィードバックを送信 20 km

1. Introduction

Muon as LFV probes

- Many muons can be available. (~10^8 /s)
- Lifetime is long. (2.2 μs)

Free muons

1) $\mu^+ \to e^+\gamma$

$\mathrm{BR} < 3.1 \times 10^{-13}$ by MEG & MEG II

Eur. Phys. J. C 84 (2024) 216.

2) $\mu^+ \to e^+e^-e^+$

$\mathrm{BR} < 1.0 \times 10^{-12}$ by SINDRUM

Nucl. Phys. B 299 (1988) 1.

Muonic atoms

3) $\mu^- N \to e^- N$

$\mathrm{BR} < 7 \times 10^{-13}$ by SINDRUM II

Eur. Phys. J. C 47 (2006) 337.

History of muonic LFV

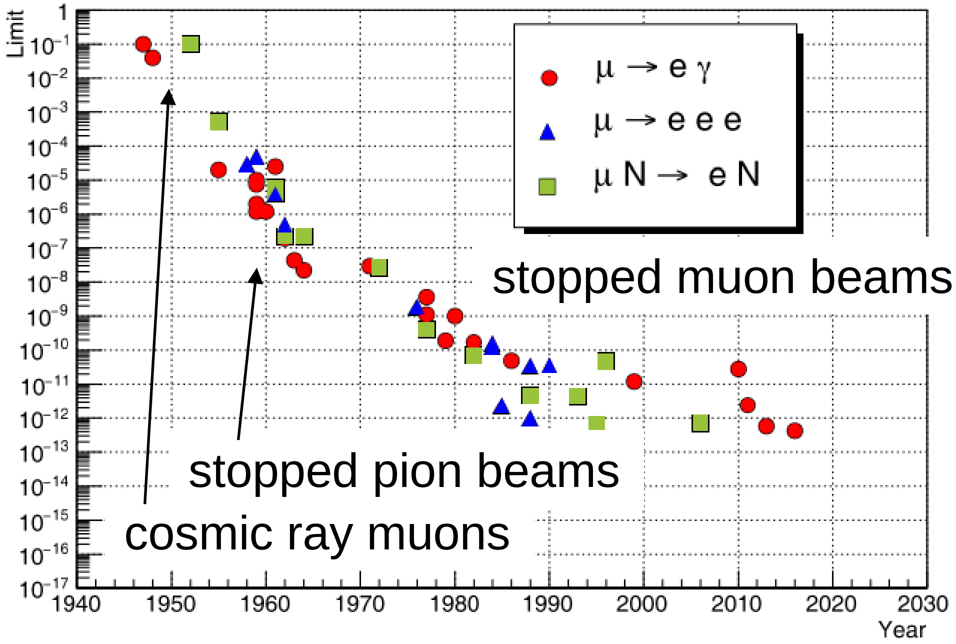

L. Calibbi & G. Signorelli, Riv. Nuovo Cim. **41**, no. 2, 1 (2018).

Muoniums

4) $\mu^+e^- \to \mu^-e^+$

$P < 8.3 \times 10^{-11}$ by MACS

(Magnetic field ~ 0.1 T) Phys. Rev. Lett. **82**, 49 (1999).

Various decays of muonic atoms

Standard processes

- $\mu^- \rightarrow e^- \nu_\mu \bar{\nu}_e$ (Decay in orbit)
- $\mu^- \rightarrow e^- \nu_\mu \bar{\nu}_e \gamma$

The spectrum near the endpoint can be BG of $\mu^- \rightarrow e^-$ conv.

- $\mu^-(Z, A) \rightarrow \nu_\mu (Z-1, A)$ (Nuclear muon capture)
- $\mu^-(Z, A) \rightarrow \nu_\mu (Z-1, A)\gamma$ (Radiative muon capture)

LFV processes

- $\mu^- \rightarrow e^-$
- $\mu^-(Z, A) \rightarrow e^+(Z-2, A)$

  "Lepton Number Violation"
  discussed in Joe Sato's talk yesterday

- $\mu^- \rightarrow e^- X$

  X: invisible boson
- $\mu^- \rightarrow e^- \gamma$
- $\mu^- e^- \rightarrow e^- e^-$

  e^- in atomic orbits

2. Calculating lepton wave functions

Bound muon & scattering electron

For calculating the $\mu^- \to e^-$ transition,

we need wave functions of the bound μ^- & the scattering e^-

to obtain the overlap integral.

(e.g., $\int dr \rho(r) \overline{\psi}_e(r) O \psi_\mu(r)$ for coherent μ-e conv.)

✓ Here, the emitted e^- w.f. is not a plane wave:

Its wave function is **distorted** by the nuclear Coulomb potential.

The formula for the decay rate gets complicated

because the electron w.f. should be expanded

by its angular momenta.

✓ In heavy nuclei, a bound muon is located near the nucleus.

Bohr radius: $\sim (m_\mu Z\alpha)^{-1} \sim 2 \times \frac{137}{Z}$ fm

Nuclear radius: $\sim 1.2 \times A^{1/3}$ fm ↔ comparable !!

⇨ It is important to consider the finite nuclear size.

Dirac equation with Coulomb potential

$$\left[i\partial_\mu\gamma^\mu - m + eA_\mu\gamma^\mu\right]\psi(\boldsymbol{r}) = 0$$

A_0 is replaced with the nuclear Coulomb potential.

$$\Rightarrow \quad E\psi(\boldsymbol{r}) = [-i\boldsymbol{\alpha}\cdot\nabla + m\beta - V(\boldsymbol{r})]\psi(\boldsymbol{r})$$

Assuming $V(\boldsymbol{r})$ is spherical, we obtain the radial Dirac equation,

$$\begin{cases} \dfrac{dg_\kappa(r)}{dr} + \dfrac{1+\kappa}{r}g_\kappa(r) - \big(E + m - V(r)\big)f_\kappa(r) = 0 \\ \dfrac{df_\kappa(r)}{dr} + \dfrac{1-\kappa}{r}f_\kappa(r) + \big(E - m - V(r)\big)g_\kappa(r) = 0 \end{cases} \qquad \psi_\kappa(r) = \begin{pmatrix} g_\kappa(r)\chi_\kappa \\ if_\kappa(r)\chi_{-\kappa} \end{pmatrix}$$

κ is the index of angular momenta: $\kappa = \begin{cases} -(l+1) & (j = l + 1/2) \\ l & (j = l - 1/2) \end{cases}$

l: orbital ang. mom. j: total ang. mom.

e.g., s-wave corresponds to $\kappa = -1$.

Calculation for bound states

- What we want: the (binding) energy & wave functions

$G(r) = rg(r)$

$F(r) = rf(r)$

Boundary conditions:

$G(0) = F(0) = 0$

$G(\infty) = F(\infty) = 0$

$$\begin{cases} \dfrac{dG_\kappa(r)}{dr} + \dfrac{\kappa}{r} G_\kappa(r) - \big(E + m - V(r)\big) F_\kappa(r) = 0 \\ \dfrac{dF_\kappa(r)}{dr} - \dfrac{\kappa}{r} F_\kappa(r) + \big(E - m - V(r)\big) G_\kappa(r) = 0 \end{cases}$$

For a given E, we can solve the differential equations from both $r = 0$ and $r = \infty$.

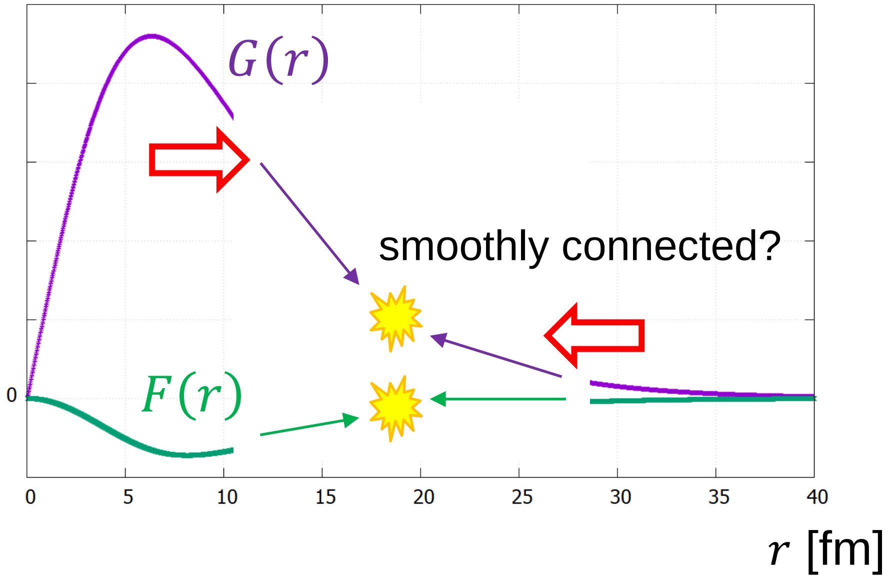

If E dose not give a bound state, the evolved function will blow up.

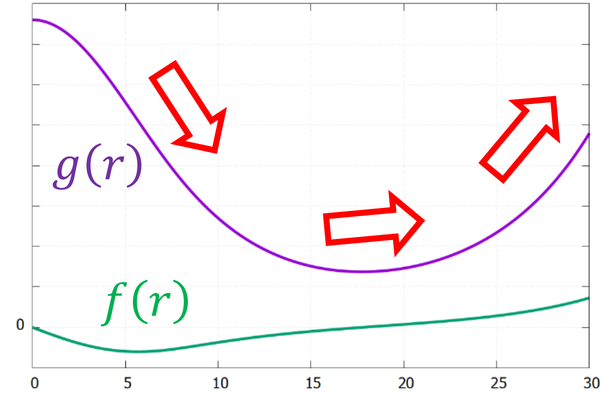

If E is appropriate, it is expected that the two curves will be smoothly connected.

Calculation for bound states

A way to find the appropriate energy to get a smooth w.f.:

Wronskian at the matching point r_m,

$$W(E) = g_{0\to m}(r_m)g'_{\infty\to m}(r_m) - g'_{0\to m}(r_m)g_{\infty\to m}(r_m)$$

(If E gives the appropriate binding energy, $W(E) = 0$.)

Step 1: Look for the zero-point of $W(E)$:

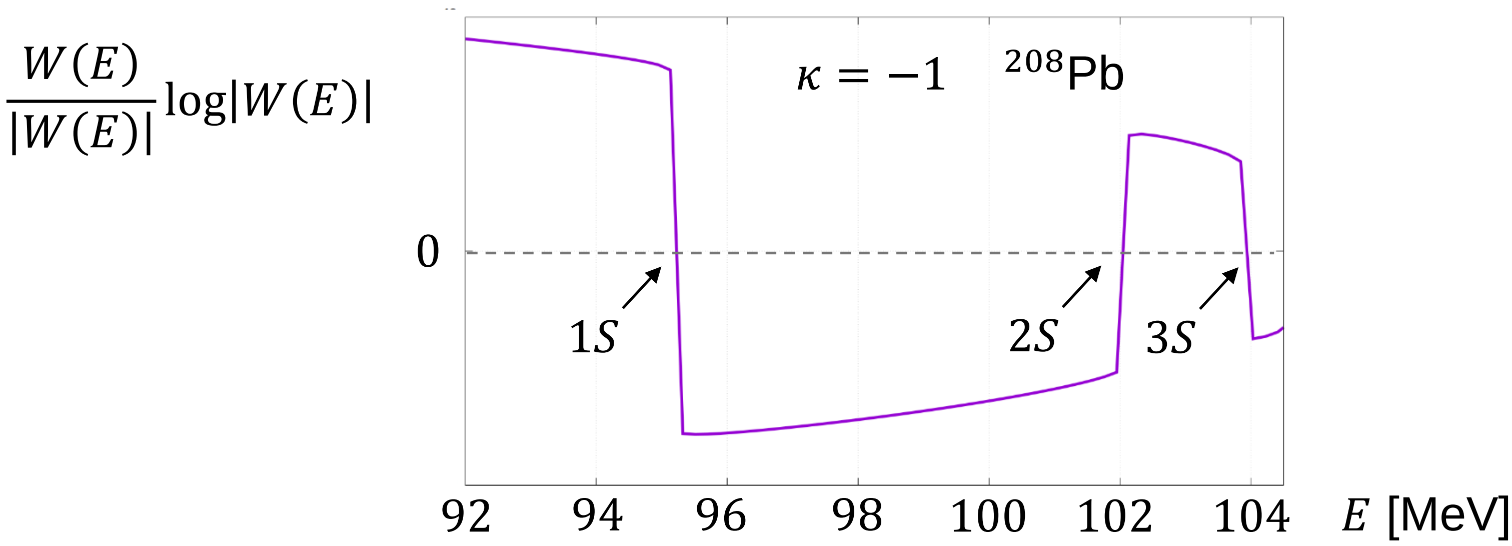

Step 2: Normalize the wave functions to satisfy the normalization condition:

$$4\pi \int_0^\infty dr\, r^2\{g(r)^2 + f(r)^2\} = 1$$

Bound wave functions

for $^{208}\mathrm{Pb}$ $(Z = 82, A = 208)$

$g(r)$ & $f(r)$ of bound μ^- (1s)

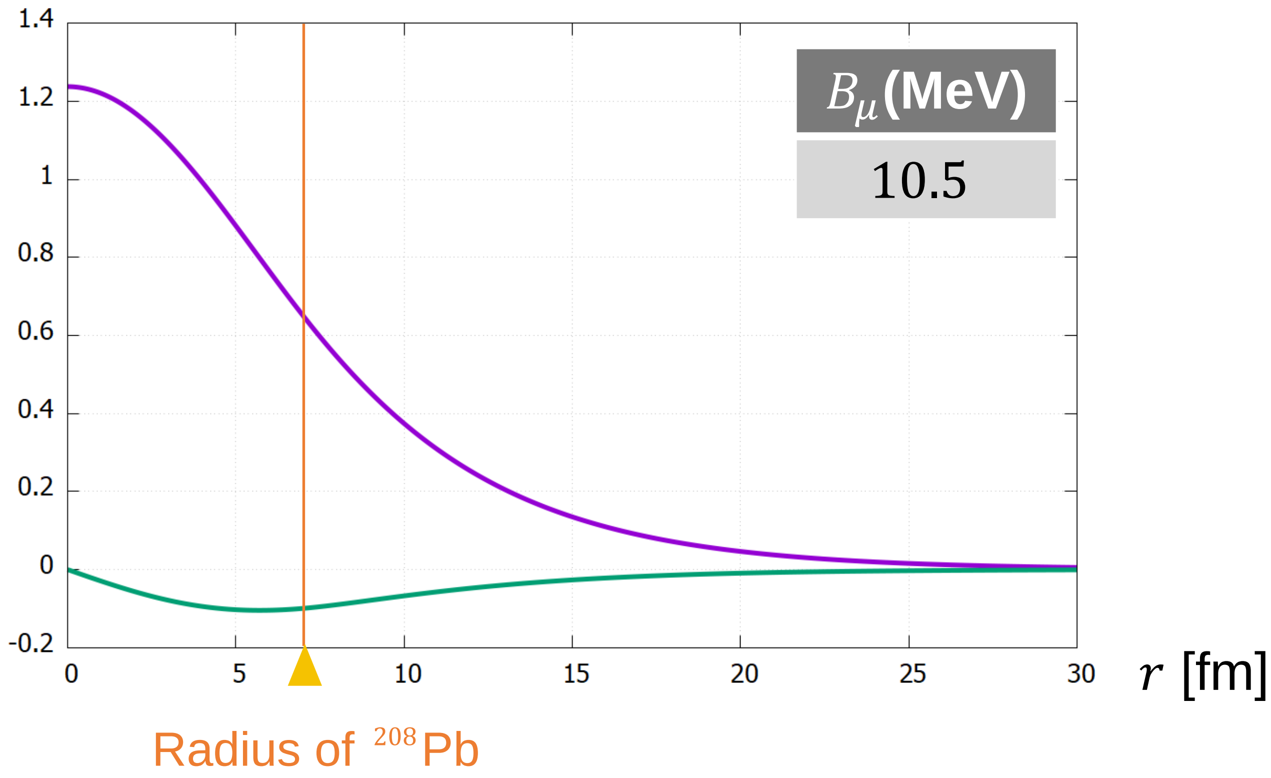

Calculation for scattering states

Since the Coulomb potential violates the translation symmetry,
the momentum is no longer a good quantum number.

Multipole expansion: $\psi_p(\boldsymbol{r}) = 4\pi \sum_\kappa i^{l_\kappa} (l_\kappa, m, 1/2, s | j_\kappa, \nu) Y_{l_\kappa}^{m*}(\hat{p}) e^{-i\delta_\kappa} \psi_\kappa(r)$

"p" indicates the boundary condition at infinity.

phase shift

- What we want: wave functions & phase shift δ for a given E

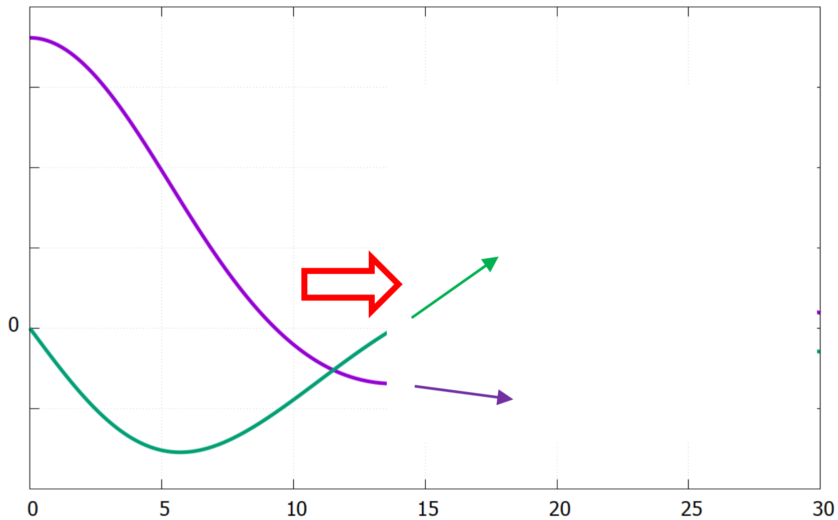

r [fm]

The normalization is determined by the boundary condition:

$$\lim_{r\to\infty} g(r) = \cos\delta\, g^{reg}(r) - \sin\delta\, g^{irr}(r)$$

$g^{reg}(r)$ & $g^{irr}(r)$:
solutions regular & irregular at $r = 0$
of Dirac eq. without the potential

Scattering wave functions

for $^{208}\mathrm{Pb}$ $(Z = 82, A = 208)$

$rg(r)$ of scattering e^-

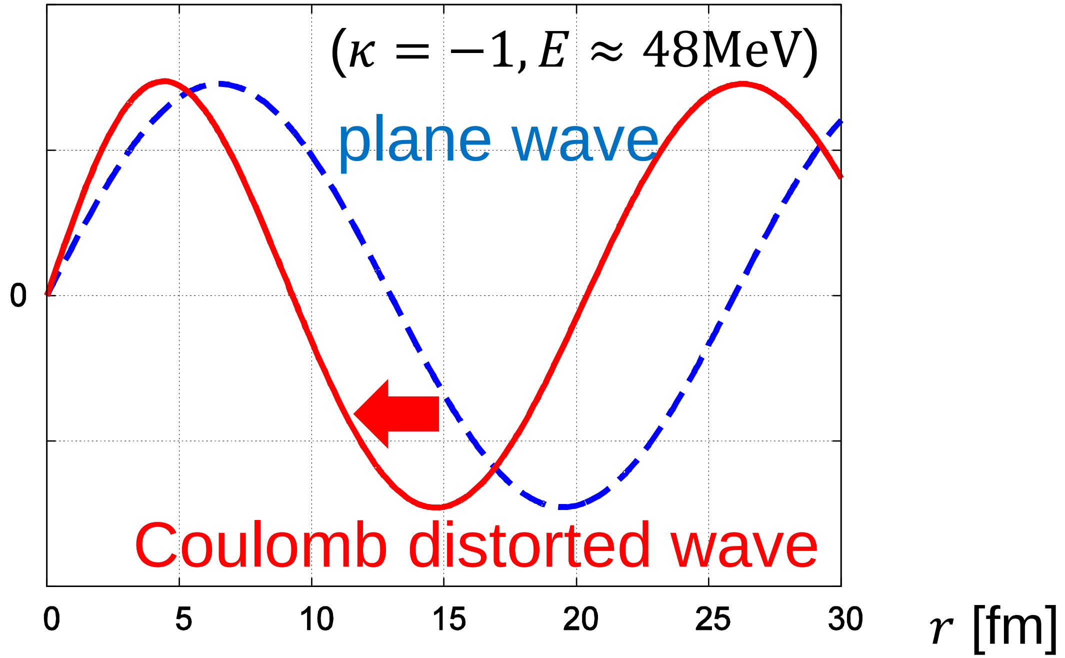

Distortion effects can be interpreted as follows:

① The value near $r = 0$ gets larger, to enhance the overlap with the bound muon.

② The effective momentum (wave number) gets larger,
to suppress the overlap with the bound muon.

3. Decay in orbit

J. Heeck, R. Szafron, & YU, PRD105, 053006; arXiv:2110.14667.

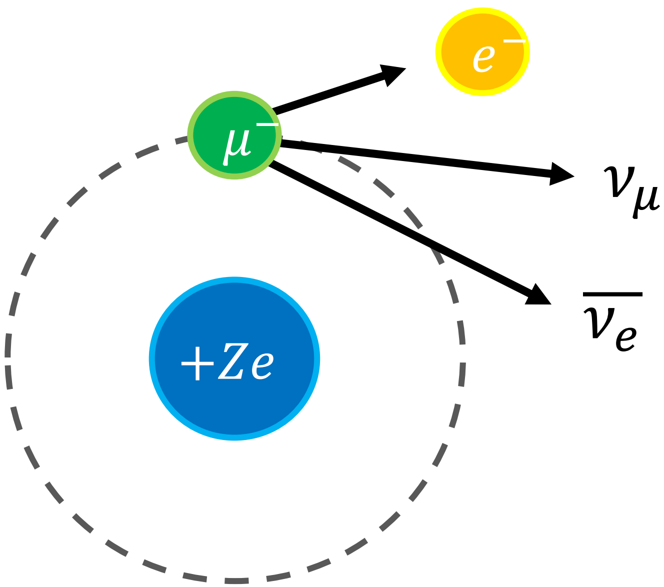

Decay in orbit (DIO)

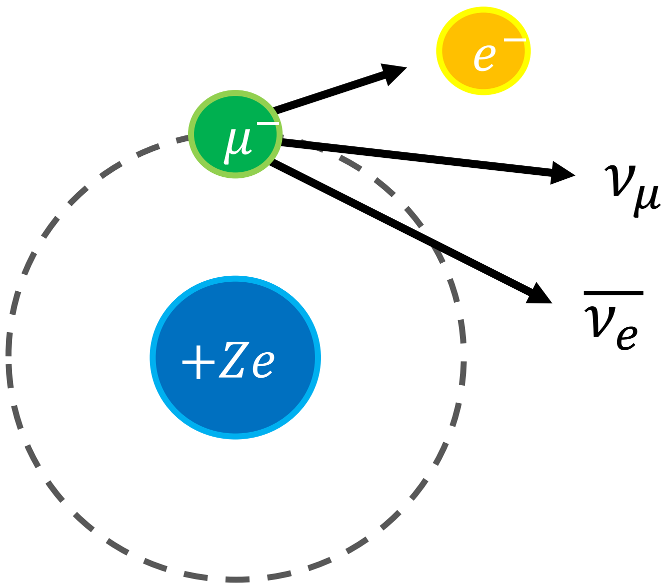

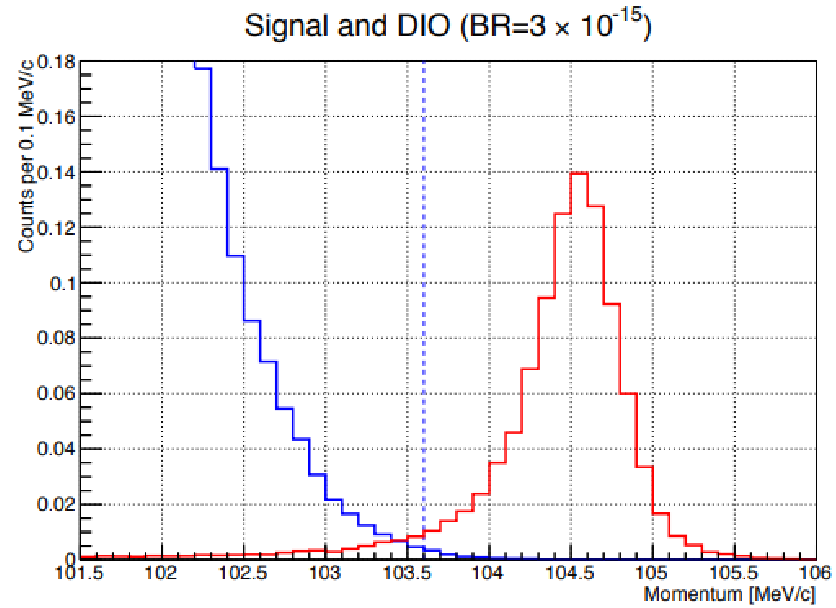

COMET technical design report, arXiv:1812.09018.

- the “standard” decay of a muon, $\mu^- \rightarrow e^- \nu_\mu \overline{\nu}_e$
- electron energy : $E_e < m_\mu - E_b - E_N$

cf. For free muons, $E_e \leq m_\mu / 2$

due to the energy-momentum conservation of a two-body decay.

For muonic atoms, the nuclear recoil makes the tail of the spectrum.

Total width of DIO

The “standard” decay width of muonic atoms is given by
the sum of the DIO width and the nuclear capture width:

$$\Gamma_{\mathrm{total}} = \Gamma_{\mathrm{DIO}} + \Gamma_{\mathrm{NC}}$$

The width of DIO slightly depends on the nuclei:

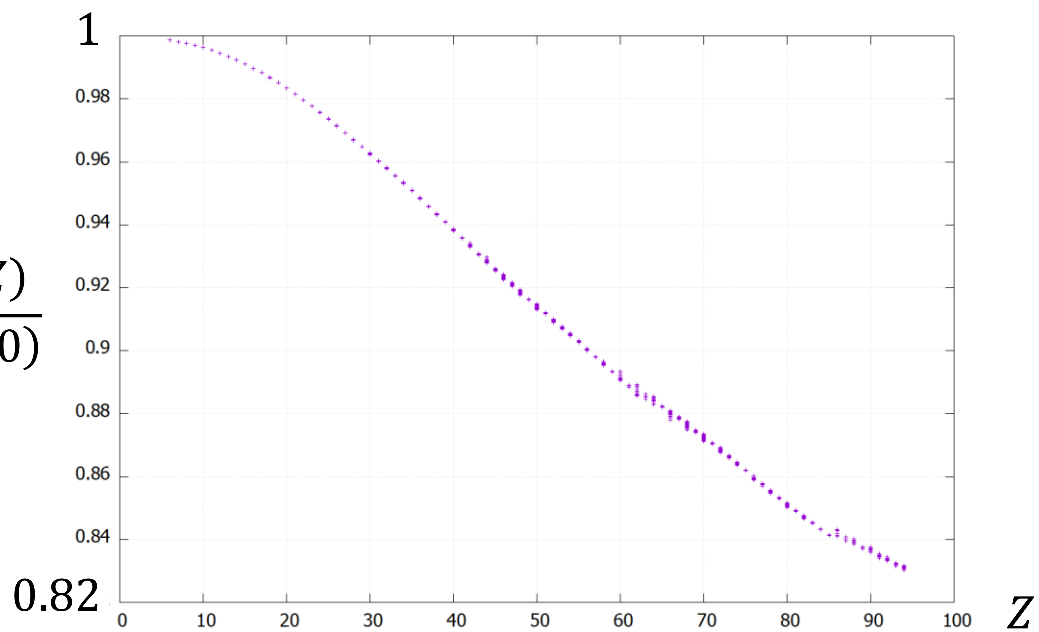

$$\frac{\Gamma_{\mathrm{DIO}}(Z)}{\Gamma(Z=0)}$$

(called “Huff factor”)

(The Huff factor is important to determine Γ_{NC} from experiments.)

Spectrum of the DIO electron

R. Watanabe *et al*. (1993).

$\mu^- \to e^- \nu_\mu \bar{\nu}_e$ process in the nuclear Coulomb field

- μ^- : bound wave ⇦ Solving Dirac eq. numerically
- e^- : distorted wave

$$\psi_\kappa(r) = \begin{pmatrix} g_\kappa(r)\chi_\kappa \\ i f_\kappa(r)\chi_{-\kappa} \end{pmatrix}$$

$$\frac{dg_\kappa(r)}{dr} + \frac{1+\kappa}{r} g_\kappa(r) - \big(E + m - V(r)\big) f_\kappa(r) = 0$$

$$\frac{df_\kappa(r)}{dr} + \frac{1-\kappa}{r} f_\kappa(r) + \big(E - m - V(r)\big) g_\kappa(r) = 0$$

- finite size of the nucleus

charge density $\rho(r)$ → potential $V(r)$

$$V(r) = -e \int_0^\infty dr' \, r'^2 \left[\frac{\theta(r - r')}{r} + \frac{\theta(r' - r)}{r'} \right] \rho(r)$$

➢ atomic number → large
- peak → shifted to low-energy side
- high energy tail → enlarged

DIO spectrum

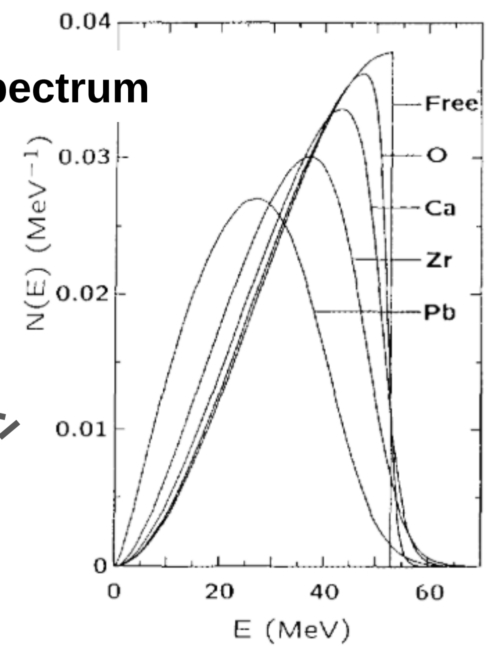

DIO spectrum

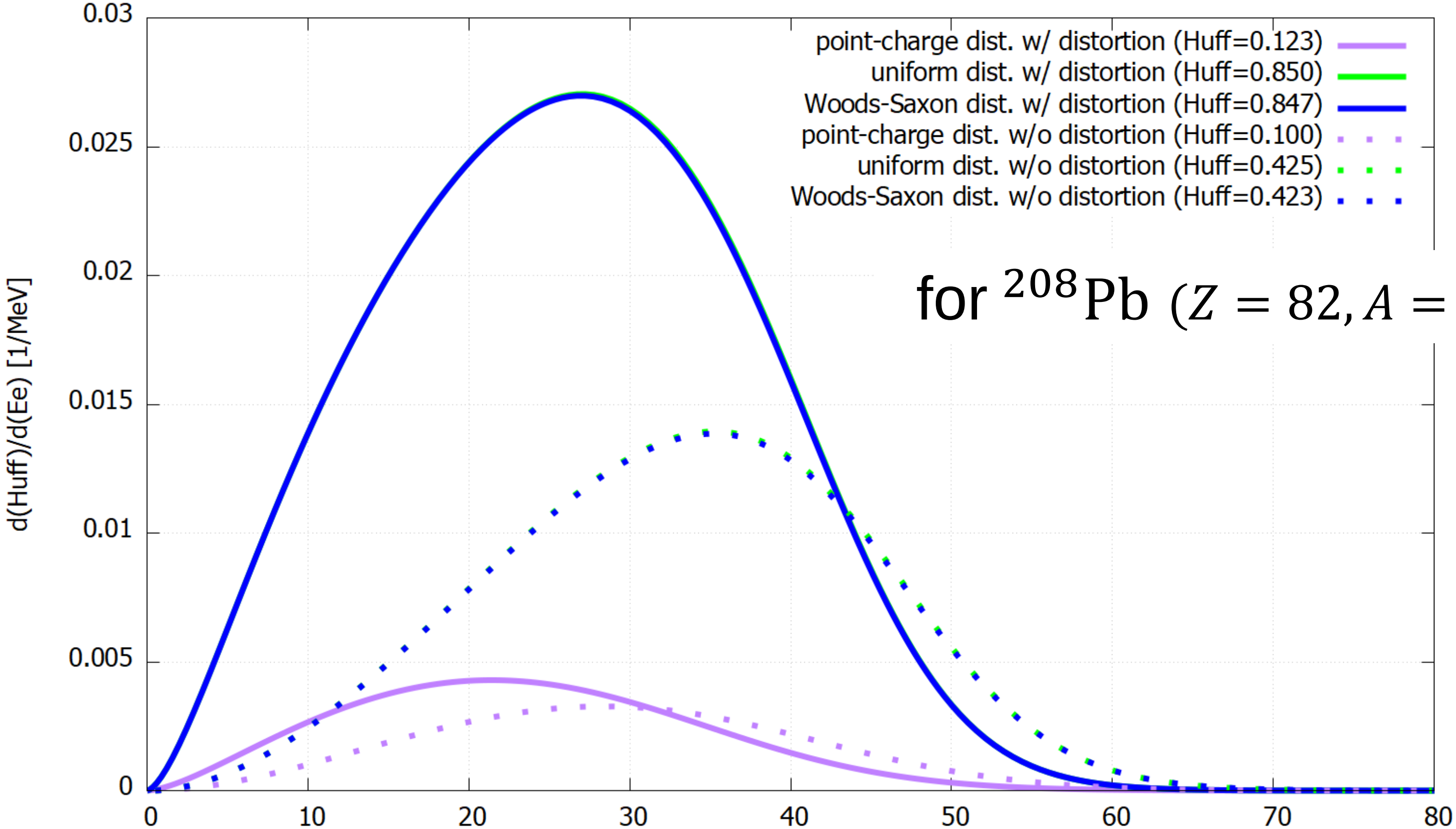

for $^{208}\mathrm{Pb}$ $(Z = 82, A = 208)$

E_e [MeV]

- ✓ Considering the finite size of the nucleus is important (unless Z is small) because the bound muon exists close to the nuclei.
- ✓ The e^{-} distortion enhances the low energy region & suppresses high energy region.

Behavior near the endpoint

important to estimate BG of $\mu^- \to e^-$ conv.

- nuclear recoil O. Shanker, PRD**25**, 1847 (1981). A. Czarnecki *et al.*, PRD**84**, 013006 (2011).

$$E_e \to E_e - \frac{E_e^2}{2m_N}$$

$$\Rightarrow E_{\rm end} = m_\mu - E_b - E_{\rm recoil}$$

$$E_{\rm recoil} = \frac{(m_\mu - E_b)^2}{2m_N}$$

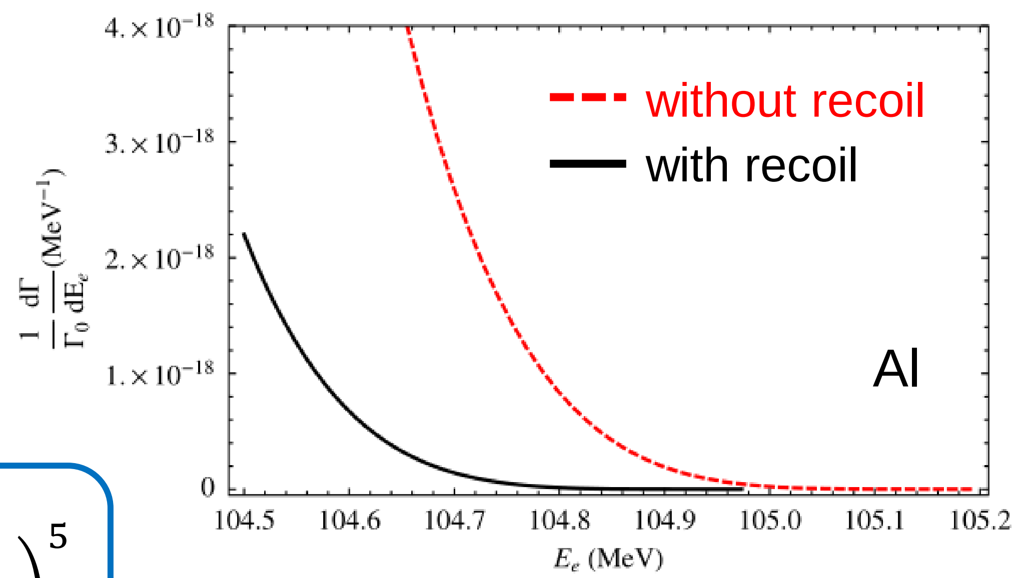

expansion near the endpoint

$$\left.\frac{1}{\Gamma_0}\frac{d\Gamma}{dE_e}\right|_{E_e \simeq E_{\rm end}} = B E_{\rm end}^5 \left(1 - \frac{E_e}{E_{\rm end}}\right)^5$$

$$B = \frac{64}{5\pi m_\mu^5}\left(p_1^2 + \frac{s_1^2}{3} + \frac{2}{3} r_2^2\right)$$

$$p_\kappa = \langle g_{-\kappa} G \rangle$$

$$s_\kappa = \langle f_{-\kappa} F \rangle$$

$$r_\kappa = \langle g_{-\kappa} F \rangle$$

g, f: electron

G, F: muon

$$\langle \cdots \rangle \equiv \int_0^\infty \cdots r^2 dr$$

κ: index of angular mom.

Radiative corrections

R. Szafron & A. Czarnecki, PRD**94**, 051301 (2016).

- vacuum polarization

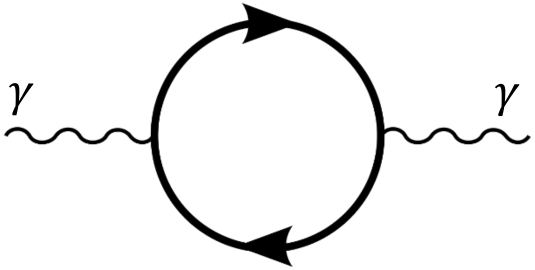

⇨ modify the nuclear potential

⇨ modify the endpoint via E_b

- soft photon radiation

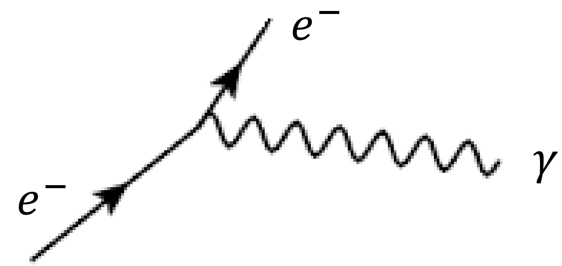

⇨ modify the shape near endpoint

$$\left.\frac{1}{\Gamma_0}\frac{d\Gamma}{dE_e}\right|_{E_e \simeq E_{\mathrm{end}}} = B E_{\mathrm{end}}^5 \left(1 - \frac{E_e}{E_{\mathrm{end}}}\right)^5 \quad \Rightarrow \quad \left.\frac{1}{\Gamma_0}\frac{d\Gamma}{dE_e}\right|_{E_e \simeq E'_{\mathrm{end}}} = B E'^5_{\mathrm{end}} \left(1 - \frac{E_e}{E'_{\mathrm{end}}}\right)^{5+\delta}$$

$$E'_{\mathrm{end}} = E_{\mathrm{end}} + \frac{\alpha m_\mu (Z\alpha)^2}{\pi}\left(\frac{11}{9} - \frac{2}{3}\log\left[\frac{2 m_\mu Z\alpha}{m_e}\right]\right) \qquad \delta = \frac{2\alpha}{\pi}\left(\log\left[\frac{2m_\mu}{m_e}\right] - 1\right) \simeq 0.023$$

Nuclear charge distribution

- measured by electron scattering

W. Boeglin *et al.*, Nucl. Phys. A **477** (1988) 399.
J. Wesseling *et al.*, PRC **55** (1997) 2773.
H. De Vries *et al.*, Atom. Data Nucl. Data Tabl. **36** (1987) 495.
G. Fricke *et al.*, Atom. Data Nucl. Data Tabl. **60** (1995) 177.
A. A. Kabir, PhD thesis, Kent State Univ., US (2015).

- Different “fitting functions” are used:

Examples of fitting funtions

1. three(two)-parameter Fermi (3pF, 2pF)

$$\rho(r) = \frac{\rho_0}{1 + \exp\frac{r-c}{z}}\left(1 + \omega\frac{r^2}{c^2}\right)$$

(2pF: $\omega = 0$)

2. there-parameter Gaussian (3pG)

$$\rho(r) = \frac{\rho_0}{1 + \exp\frac{r^2-c^2}{z^2}}\left(1 + \omega\frac{r^2}{c^2}\right)$$

3. modified-harmonic oscillator (MHO)

$$\rho(r) = \rho_0\left(1 + \omega\frac{r^2}{a^2}\right)\exp\left(-\frac{r^2}{a^2}\right)$$

4. Fourier-Bessel (FB)

5. Sum of Gaussians (SOG)

- There are nuclides which has only data of “radius”. ← we assume 1pF dist.

I. Angeli & K. P. Marinova, Atom. Data Nucl. Data Tabl. **99** (2013) 69.

$$\rho(r) = \frac{\rho_0}{1 + \exp\frac{r-c}{0.52\ \mathrm{fm}}}$$

Numerical results

Table of E'_{end} & B for various nuclides and models

	$E'_{\text{end}}/\text{MeV}$	$B_{1\text{pF}}/\text{MeV}^{-6}$	$B_{\text{FB}}/\text{MeV}^{-6}$	$B_{\text{SOG}}/\text{MeV}^{-6}$	$B_{\text{MHO}}/\text{MeV}^{-6}$	$B_{3\text{pF}}/\text{MeV}^{-6}$	$B_{3\text{pG}}/\text{MeV}^{-6}$
${}^{4}_{2}\text{He}$	104.150			2.53×10^{-20}			
${}^{6}_{3}\text{Li}$	104.637	1.20×10^{-19}	1.29×10^{-19}				
${}^{7}_{3}\text{Li}$	104.779	1.28×10^{-19}			1.31×10^{-19}		
${}^{9}_{4}\text{Be}$	104.949	4.97×10^{-19}			4.96×10^{-19}		
${}^{10}_{5}\text{B}$	104.99	1.52×10^{-18}	1.56×10^{-18}		1.50×10^{-18}		
${}^{11}_{5}\text{B}$	105.044	1.53×10^{-18}			1.52×10^{-18}		
${}^{12}_{6}\text{C}$	105.059	3.55×10^{-18}	3.53×10^{-18}	3.55×10^{-18}			
${}^{13}_{6}\text{C}$	105.097	3.56×10^{-18}			3.63×10^{-18}		
${}^{14}_{7}\text{N}$	105.094	7.04×10^{-18}				7.13×10^{-18}	
${}^{16}_{8}\text{O}$	105.106	1.22×10^{-17}	1.19×10^{-17}	1.20×10^{-17}	1.19×10^{-17}		
${}^{19}_{9}\text{F}$	105.118	1.85×10^{-17}				1.87×10^{-17}	
${}^{20}_{10}\text{Ne}$	105.081	2.79×10^{-17}				2.87×10^{-17}	
${}^{22}_{10}\text{Ne}$	105.108	2.89×10^{-17}				2.89×10^{-17}	
${}^{23}_{11}\text{Na}$	105.063	4.35×10^{-17}					
${}^{24}_{12}\text{Mg}$	105.011	6.17×10^{-17}		6.29×10^{-17}		6.10×10^{-17}	

⋮

J. Heeck, R. Szafron, & YU, PRD105, 053006; arXiv:2110.14667.

E_b & E'_{end}

E_b/MeV

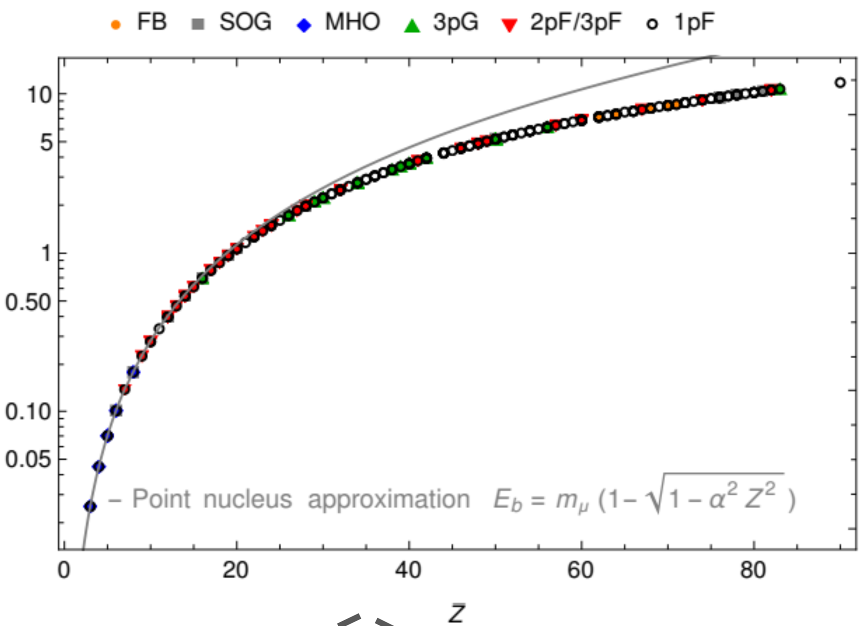

E'_{end}/MeV

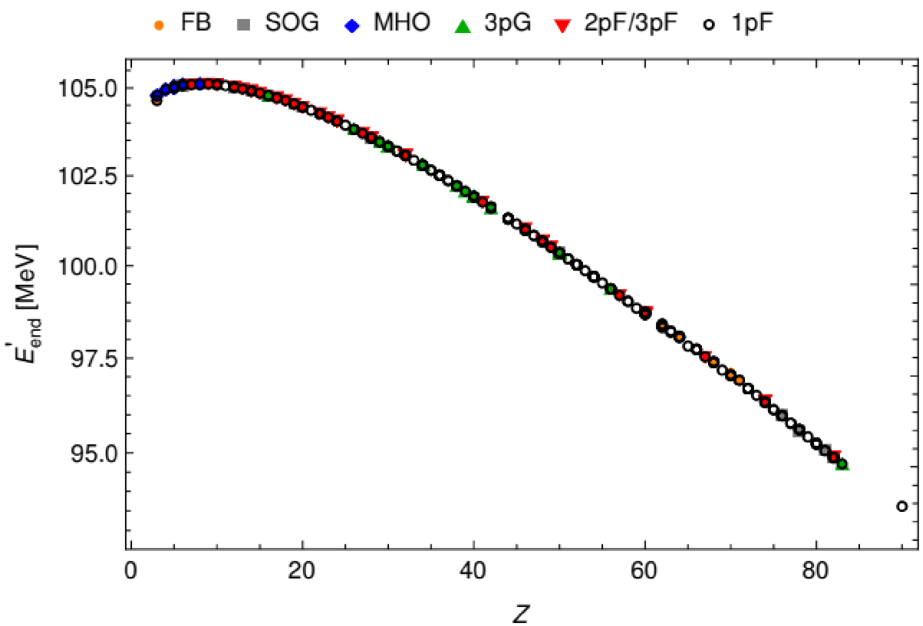

- $E_b = m_\mu\left(1 - \sqrt{1 - \alpha^2 Z^2}\right)$ for $Z < 20$, $E_b = m_\mu(-3.93 + 0.21Z)\alpha$ for $Z > 50$
- uncertainty from difference of fitting functions is less than %.
- difference of isotopes is at most 10%

B coefficient

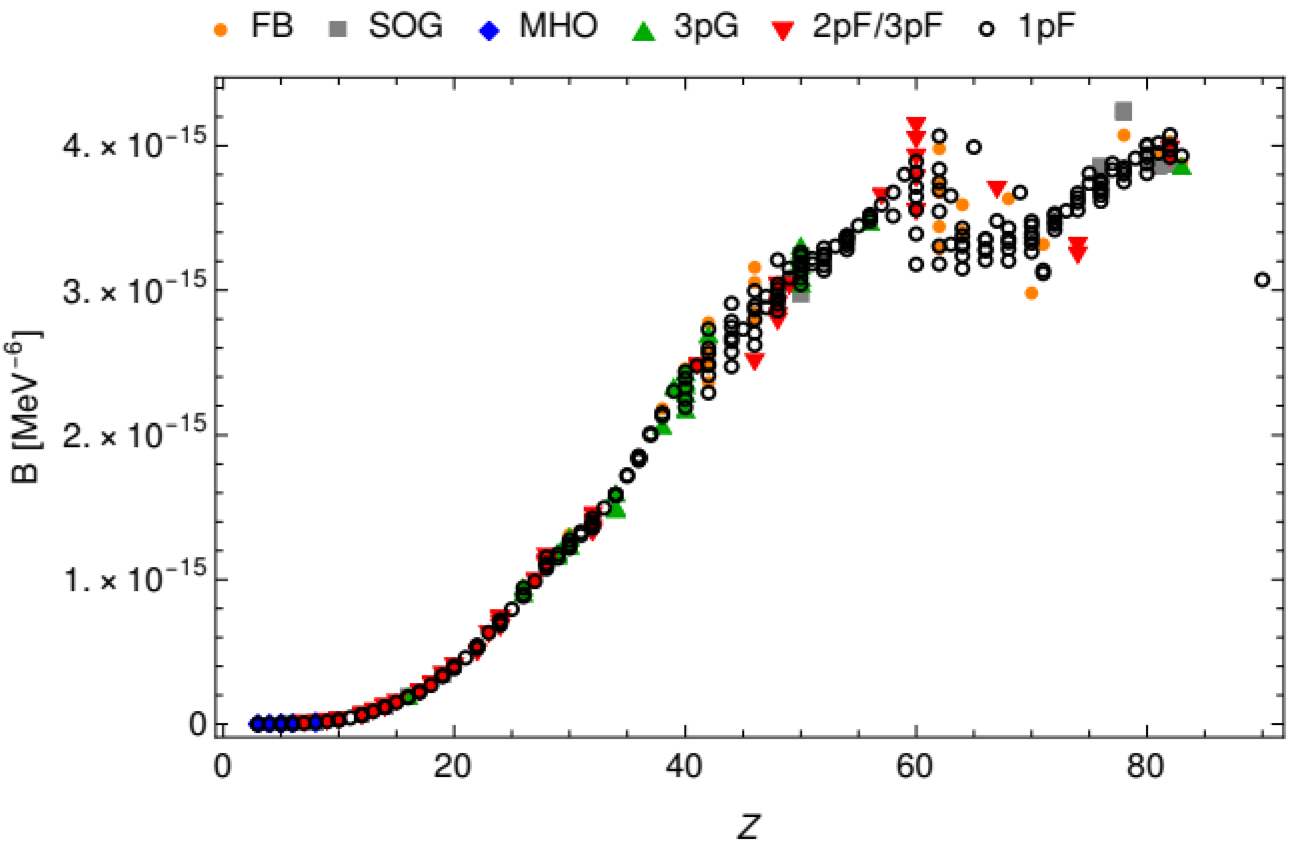

- ➢ The uncertainty from fitting functions is about 10%.
- ➢ The isotope differences are often of the same order or even larger than the uncertainty.
- ➢ How large is the quadrupole deformation effects?

4. μ-e conversion

J. Heeck, R. Szafron, & YU, NPB980, 115833; arXiv:2203.00702.

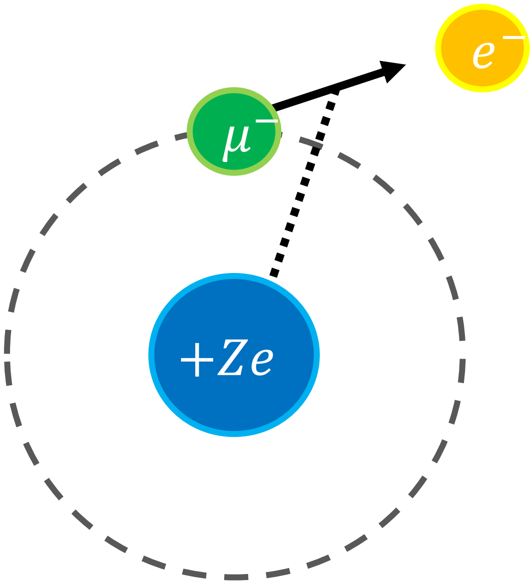

(Coherent) $\mu^- \to e^-$ conversion

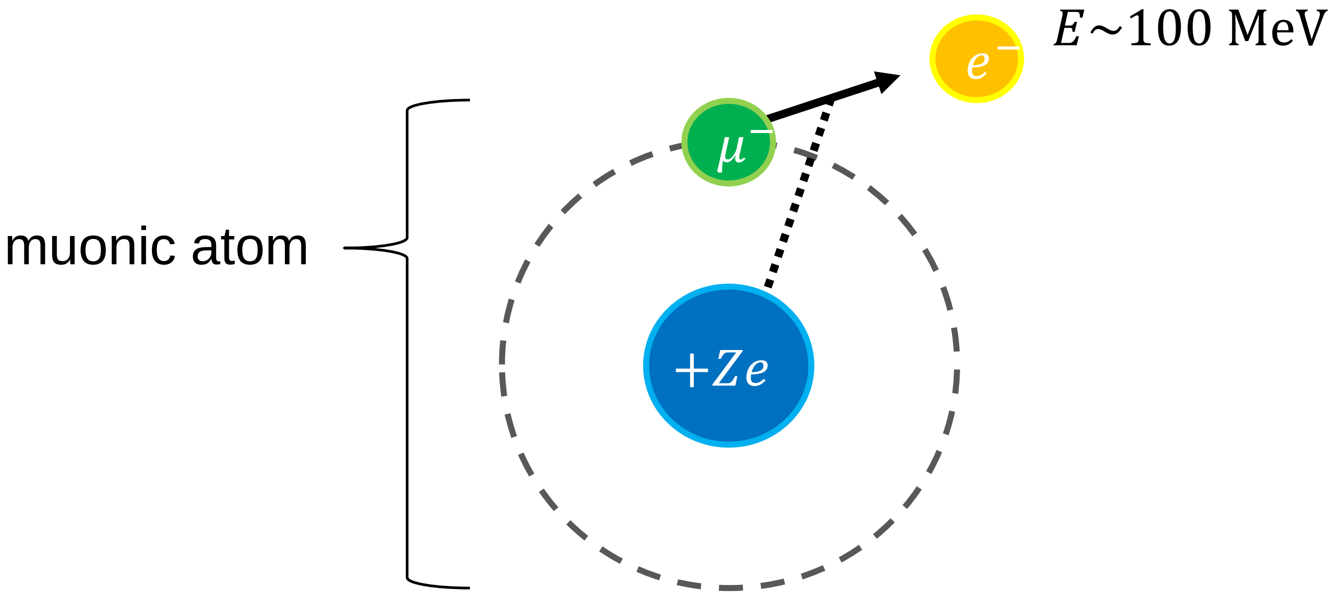

- charged lepton flavor violating (CLFV) process
- the energy of emitted e^- : $E_e = m_\mu - E_b - E_{\mathrm{recoil}} \sim 105$ MeV

E_b : binding energy of muon ~ 0.5 MeV
E_{recoil} : nuclear recoil energy ~ 0.2 MeV

for Al

Effective Lagrangian beyond the SM

$$\mathcal{L}_{\mu e} = -\frac{4G_F}{\sqrt{2}} \sum_{X=L,R} [m_\mu C_{D,X} \bar{e} \sigma^{\alpha\beta} P_X \mu F_{\alpha\beta}$$

dipole interaction

$$+ \sum_{N=p,n} \left(C_{S,X}^{(N,N)} \bar{e} P_X \mu \bar{N} N + C_{V,X}^{(N,N)} \bar{e} \gamma^\alpha P_X \mu \bar{N} \gamma_\alpha N \right)] + h.c.$$

scalar interaction

vector interaction

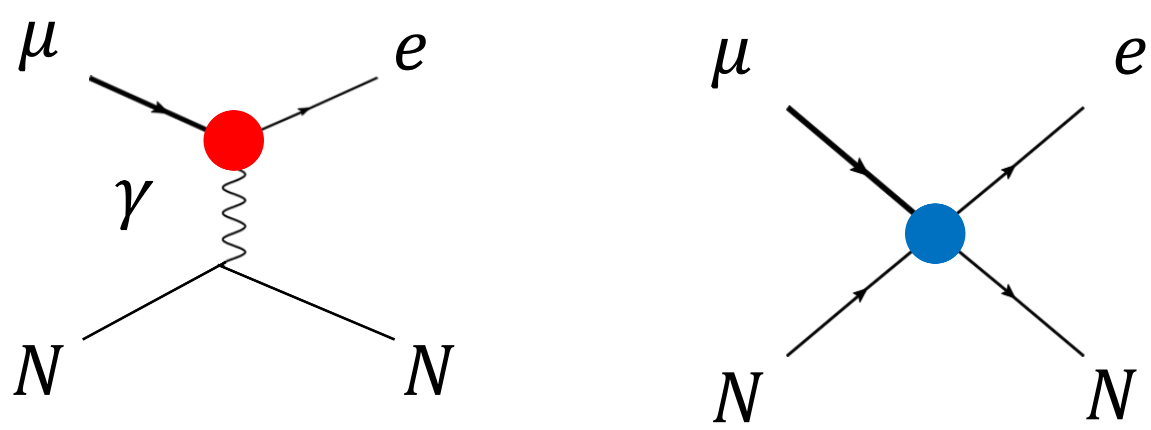

Branching ratio

R. Kitano *et al.*, PRD**84**, 013006 (2011).

$$BR_{\rm SI} = \frac{32G_F^2}{\Gamma_{\rm capture}}\left[\left|C_{D,L}\frac{D}{4} + \sum_{N=p,n}\left(C_{S,L}^{NN}S^{(N)} + C_{V,R}^{NN}V^{(N)}\right)\right|^2 + \{L \leftrightarrow R\}\right]$$

- overlap integrals

$$D = \frac{4m_\mu}{\sqrt{2}}\int_0^\infty dr\, r^2[-E(r)]\left(g_e^- f_\mu^- + f_e^- g_\mu^-\right)$$

electric field

$$S^{(p)} = \frac{1}{2\sqrt{2}}\int_0^\infty dr\, r^2 Z\rho^{(p)}\left(g_e^- g_\mu^- - f_e^- f_\mu^-\right)$$

$\rho^{(p)}$: proton density

$$S^{(n)} = \frac{1}{2\sqrt{2}}\int_0^\infty dr\, r^2 N\rho^{(n)}\left(g_e^- g_\mu^- - f_e^- f_\mu^-\right)$$

$\rho^{(n)}$: neutron density

$$V^{(p)} = \frac{1}{2\sqrt{2}}\int_0^\infty dr\, r^2 Z\rho^{(p)}\left(g_e^- g_\mu^- + f_e^- f_\mu^-\right)$$

$$V^{(n)} = \frac{1}{2\sqrt{2}}\int_0^\infty dr\, r^2 N\rho^{(p)}\left(g_e^- g_\mu^- + f_e^- f_\mu^-\right)$$

Overlap integrals (dipole integral D)

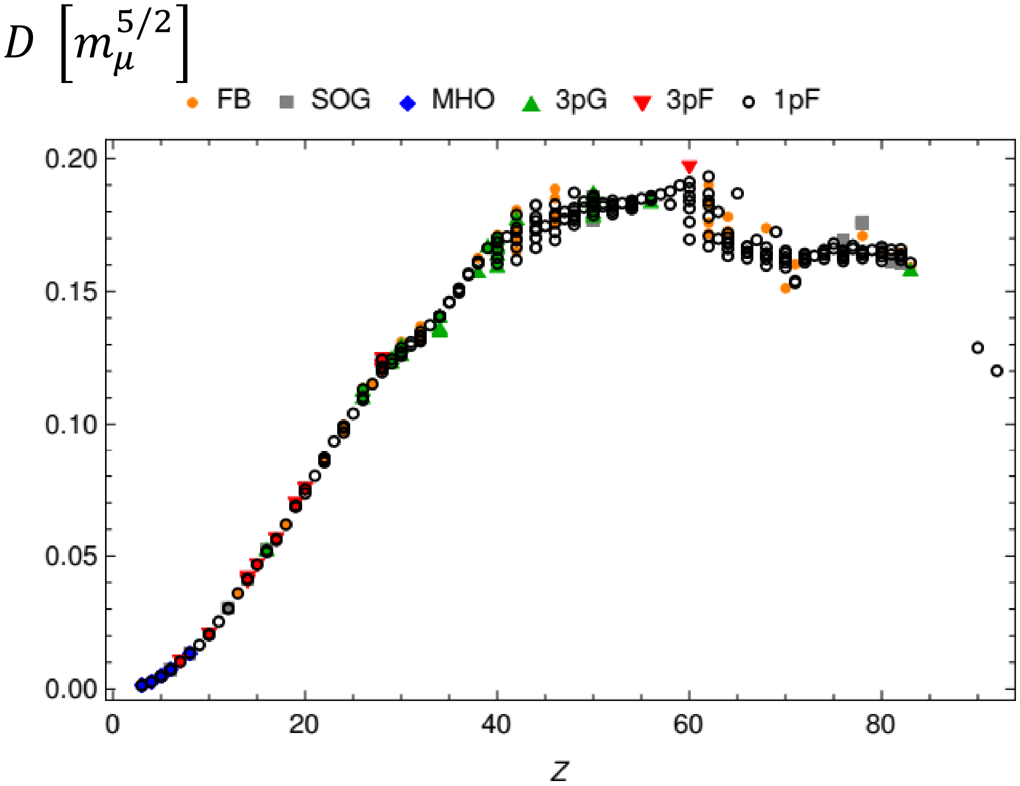

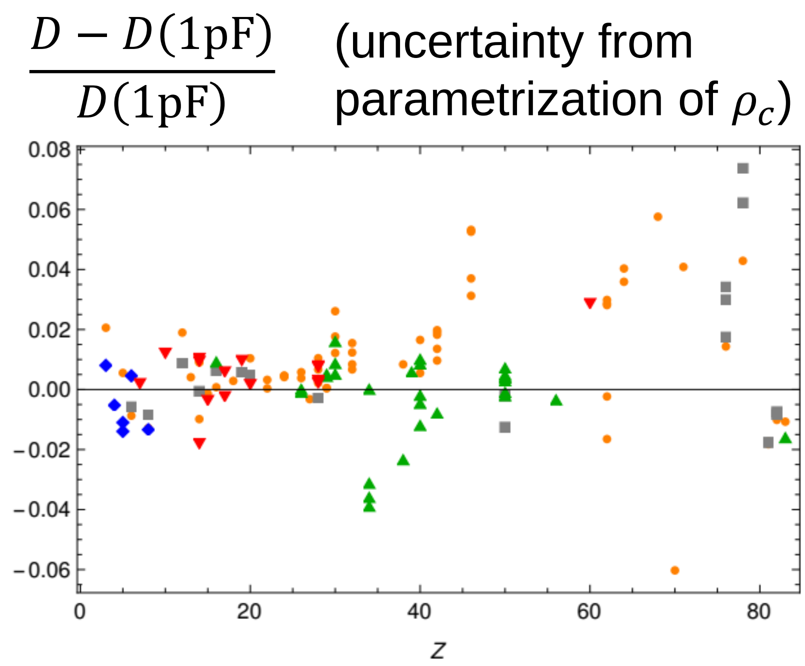

- For $Z < 30$, the uncertainty due to ρ_c is less than 2%, but grows to 8% for large Z.
- Isotope dependence exceeds the uncertainty at medium Z.

Overlap integrals

($\rho^{(n)} = \rho^{(p)}$ is assumed.)

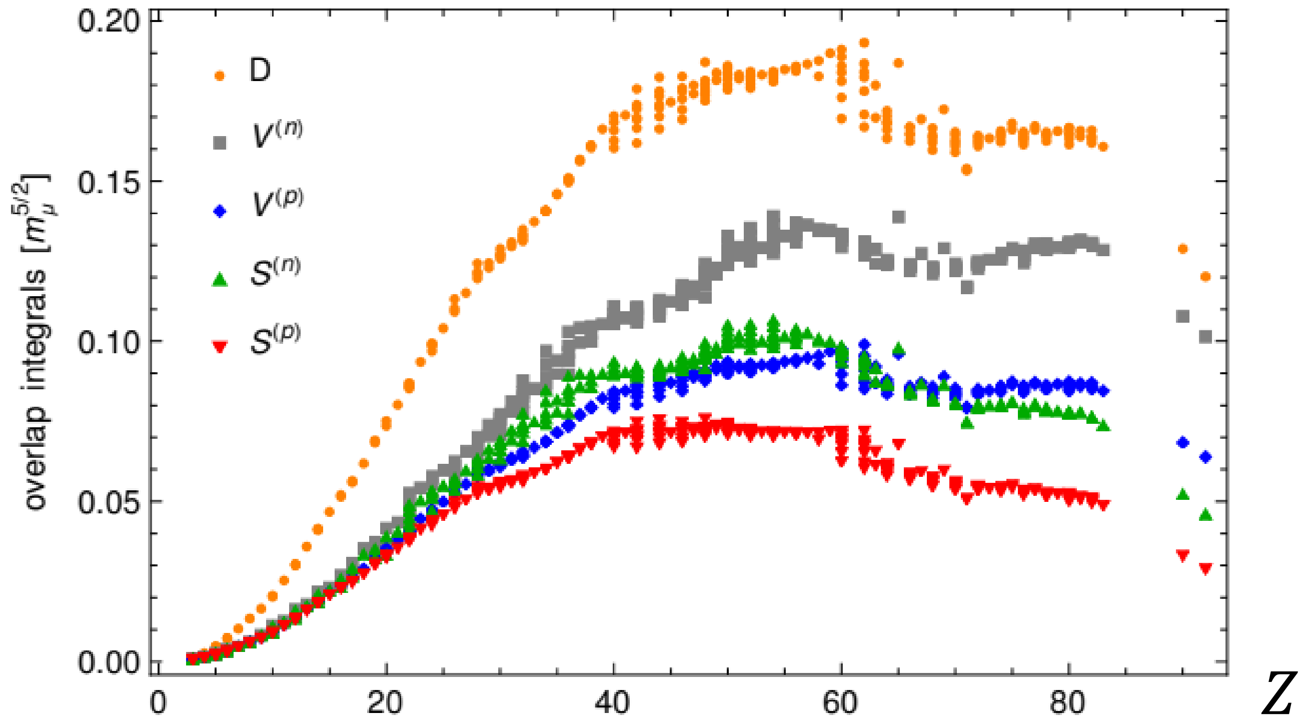

- For $S^{(p)}$ and $V^{(p)}$, the uncertainty is estimated to range from 5% at low Z to 10% at high Z.
- For $S^{(n)}$ and $V^{(n)}$, the uncertainty is also 5% at low Z, but more than 10% at high Z.

Quadrupole deformation

L. Borrel, D. G. Hitlin, S. Middleton, arXiv:2401.15025

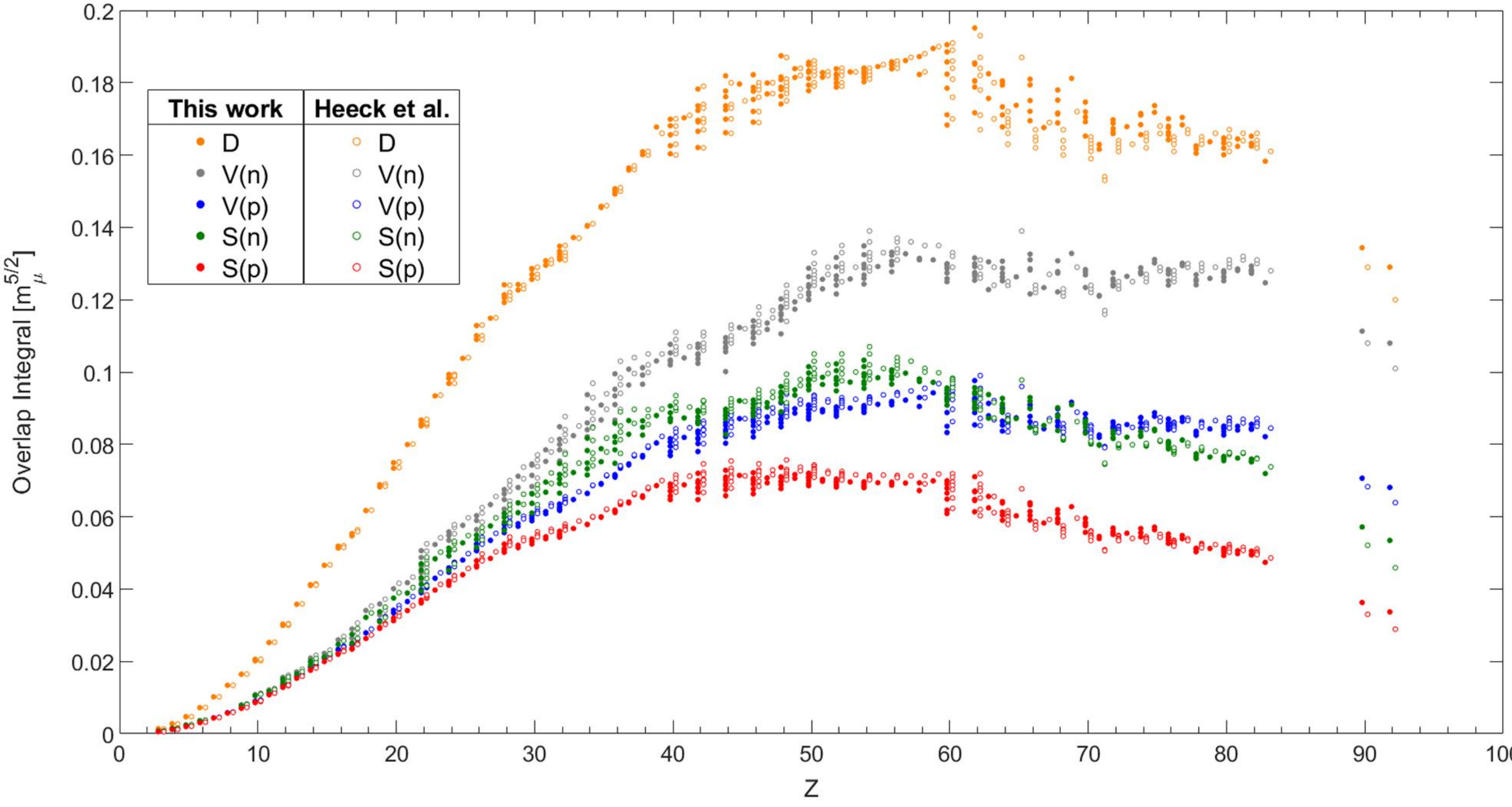

(also shown yesterday by A. Czarnecki)

Complementarity of targets

cf. S. Davidson, Y. Kuno, & M. Yamanaka, PLB790 (2019) 380.

$$BR_{\mathrm{SI}} = \frac{32G_F^2}{\Gamma_{\mathrm{capture}}}\left[|\boldsymbol{v}\cdot\boldsymbol{C}_L|^2 + |\boldsymbol{v}\cdot\boldsymbol{C}_R|^2\right]$$

$$\boldsymbol{C}_L = \left(C_{D,R}, C_{V,L}^{pp}, C_{S,R}^{pp}, C_{V,L}^{nn}, C_{S,R}^{nn}\right)$$

coefficient-space vector :

$$\boldsymbol{v} = \left(\frac{D}{4}, V^{(p)}, S^{(p)}, V^{(n)}, S^{(n)}\right)$$

If their directions of $\boldsymbol{v}$ are different, these targets are “complimentary”.

misalignment angle : $\theta_{\mathrm{Al}} = \arccos\left(\frac{\boldsymbol{v}\cdot\boldsymbol{v}_{\mathrm{Al}}}{|\boldsymbol{v}||\boldsymbol{v}_{\mathrm{Al}}|}\right)$

⇨ Large θ_{Al} means high complimentarity to Al.

Complementarity of targets

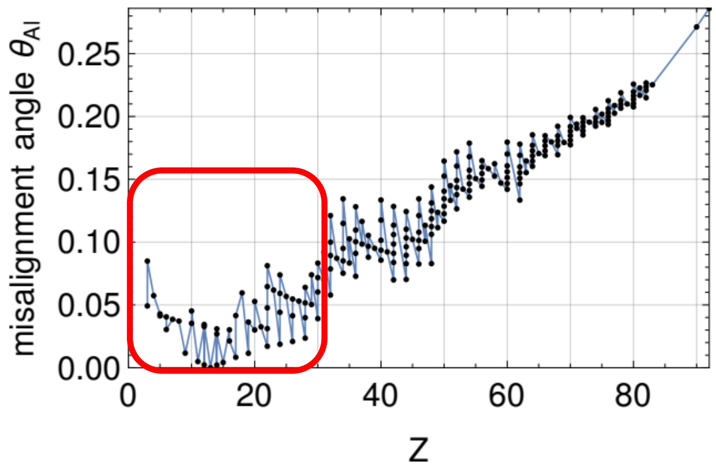

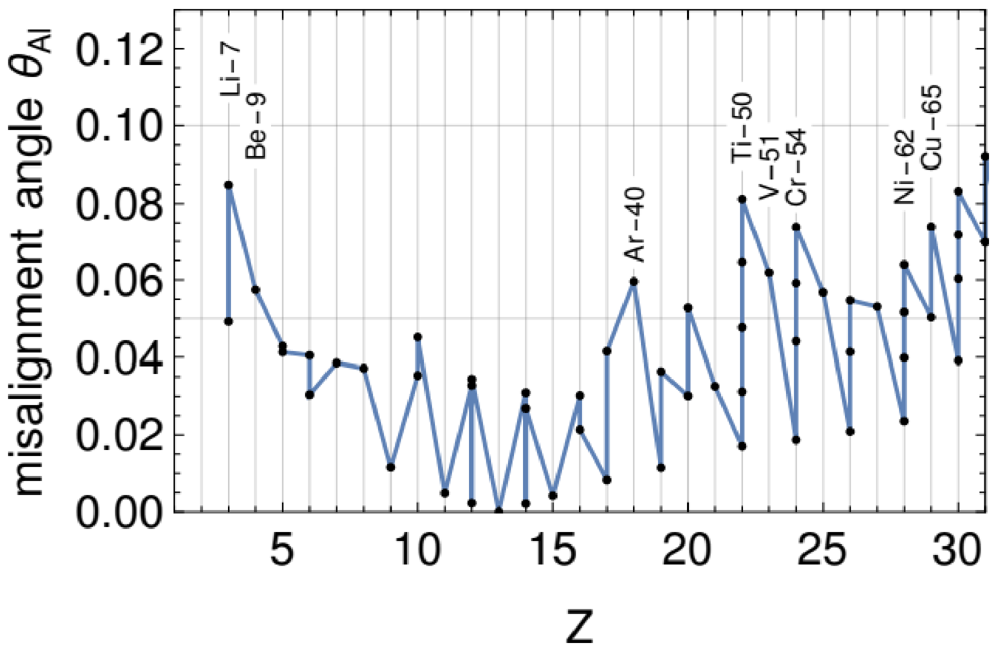

- High-Z targets have large complementary with Al.
- Low-Z targets Li-7, Ti-50 have large θ_{Al}.

cf. $A/Z = 2.33$ for Li-7

$A/Z = 2.27$ for Ti-50

($A/Z = 2.08$ for Al-27)

- Ti would be a suitable next target for Al-based experiment ?

cf. Ti-50, Ti-49, Cr-54 : natural abundance low

Li-7, V-51 : ← (practically preferable?) natural abundance >90%

5. Other LFV processes

Other LFV processes in muonic atoms

- $\mu^- \to e^- X$

X. G. i Tormo, D. Bryman, A. Czarnecki, & M. Dowling, PRD84, 113010; arXiv:1110.2874.

YU, PRD102, 095007; arXiv:2005.07894.

- $\mu^- \to e^- \gamma$

YU, M. Yamanaka, & Y. Kuno, PRD111, 035017; arXiv:2411.10304.

- $\mu^- e^- \to e^- e^-$

M. Koike, Y. Kuno, J. Sato, & M. Yamanaka, PRL105, 121601; arXiv:1003.1578.

YU, Y. Kuno, J. Sato, T. Sato, & M. Yamanaka, PRD93, 076006; arXiv:1603.01522.

YU, Y. Kuno, J. Sato, T. Sato, & M. Yamanaka, PRD97, 015017; arXiv:1711.08979.

Y. Kuno, J. Sato, T. Sato, YU, & M. Yamanaka, PRD100, 075012; arXiv:1908.11653.

5-1. $\mu^- \rightarrow e^- X$

YU, PRD102, 095007; arXiv:2005.07894.

$\mu^+ \to e^+ X$ searches

- A. Jodidio *et al.* PRD **34**, 1967 (1986).
  - $1.8 \times 10^7\ \mu^+$ that was highly polarized
  - search for e^+ emitted in opposite direction for μ^+ polarization
  - $\mathrm{Br}(\mu^+ \to e^+ X)\ <\ 2.6 \times 10^{-6}$ for $m_X = 0$

- TWIST Collab. PRD **91**, 052020 (2015).
  - $5.8 \times 10^8\ \mu^+$
  - for various m_X & various angular property ($\mathrm{d}\Gamma/\mathrm{d}\cos\theta \propto 1 - AP_\mu \cos\theta$)
  - $\mathrm{Br} < 2.1 \times 10^{-5}$ ($m_X = 0, A = 0$)

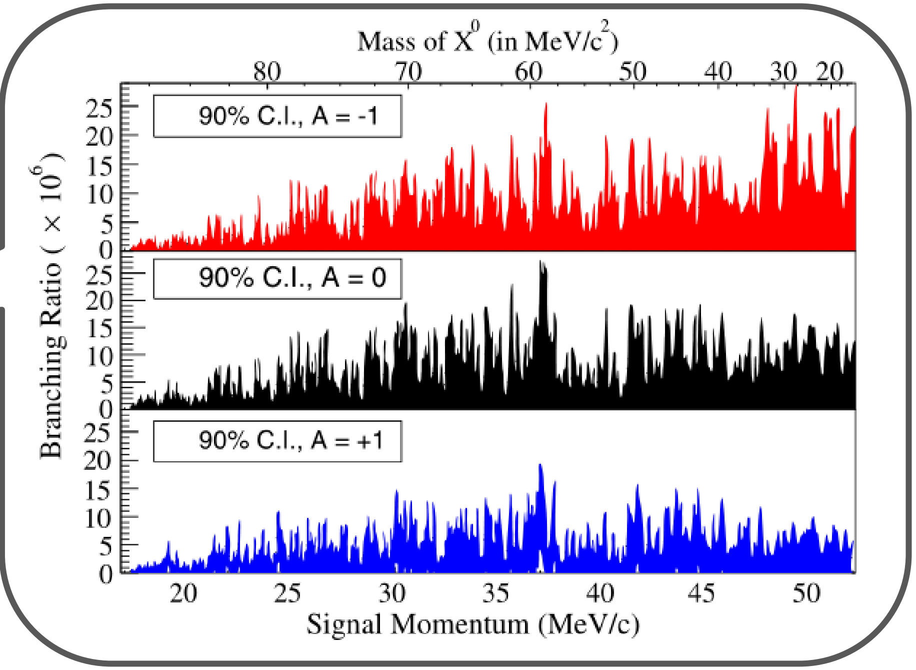

- Mu3e Collab. A. Schöning, Talk at Flavour and Dark Matter Workshop, Heidelberg, September 28 (2017).
  - $\mathrm{Br} < 10^{-8}$ (for $25\mathrm{MeV} < m_X < 95\mathrm{MeV}$)

$\mu^- \to e^- X$ in a muonic atom

originally proposed by X. G. i Tormo *et al.*, PRD **84**, 113010 (2011).

Advantages over free muon decay

1. less background

- - - : $\mu^+ \to e^+ X$ (free)
- - - : $\mu^+ \to e^+ \nu_e \bar{\nu}_\mu$ (free)
— : $\mu^- \to e^- X$ (μ-gold)
— : $\mu^- \to e^- \bar{\nu}_e \nu_\mu$ (μ-gold)

- different peak positions of signal & BG

shape of electron spectrum

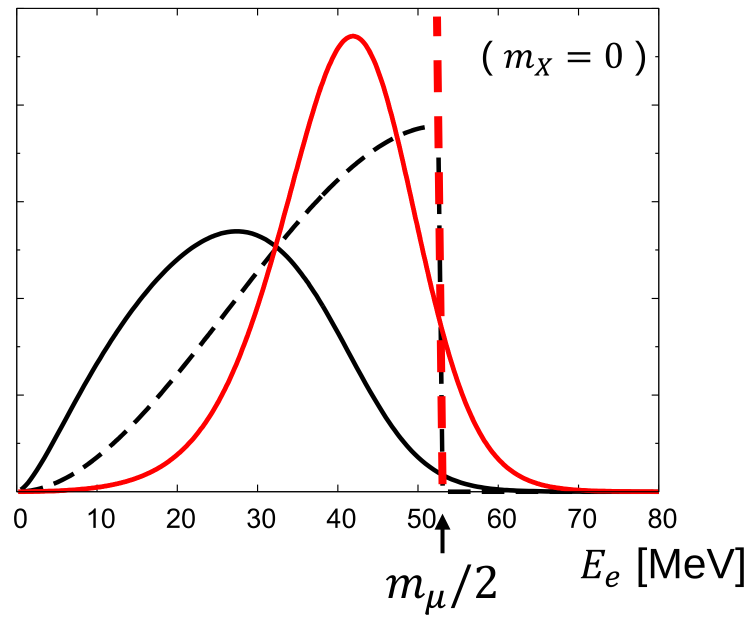

2. more information : "spectrum", "dependence on nucleus", …

3. huge # of muonic atoms in coming experiments (COMET, Mu2e, DeeMe)

Disadvantages

✓ non-monochromatic signal

✓ shorter lifetime of muonic atom

Effective models

A. **Scalar *X***

- yukawa coupling (e.g. majoron induced by R-parity violation, …)

also analyzed by X. G. i Tormo *et al.*, PRD **84**, 113010 (2011).

$$\mathcal{L}_{S0} = g_{S0}(\overline{e}\mu)X + [H.c.]$$

- derivative coupling (e.g. majoron, familon, axion, …)

$$\mathcal{L}_{S1} = \frac{g_{S1}}{\Lambda_{S1}}(\overline{e}\gamma_{\alpha}\mu)\partial^{\alpha}X + [H.c.]$$

B. **Vector *X***

- dipole coupling

$$\mathcal{L}_{V1} = \frac{g_{V1}}{\Lambda_{V1}}(\overline{e}\sigma_{\alpha\beta}\mu)X^{\alpha\beta} + [H.c.]$$

$$X^{\alpha\beta} = \partial^{\alpha}X^{\beta} - \partial^{\beta}X^{\alpha}$$

e^- spectrum ($m_X = 0$)

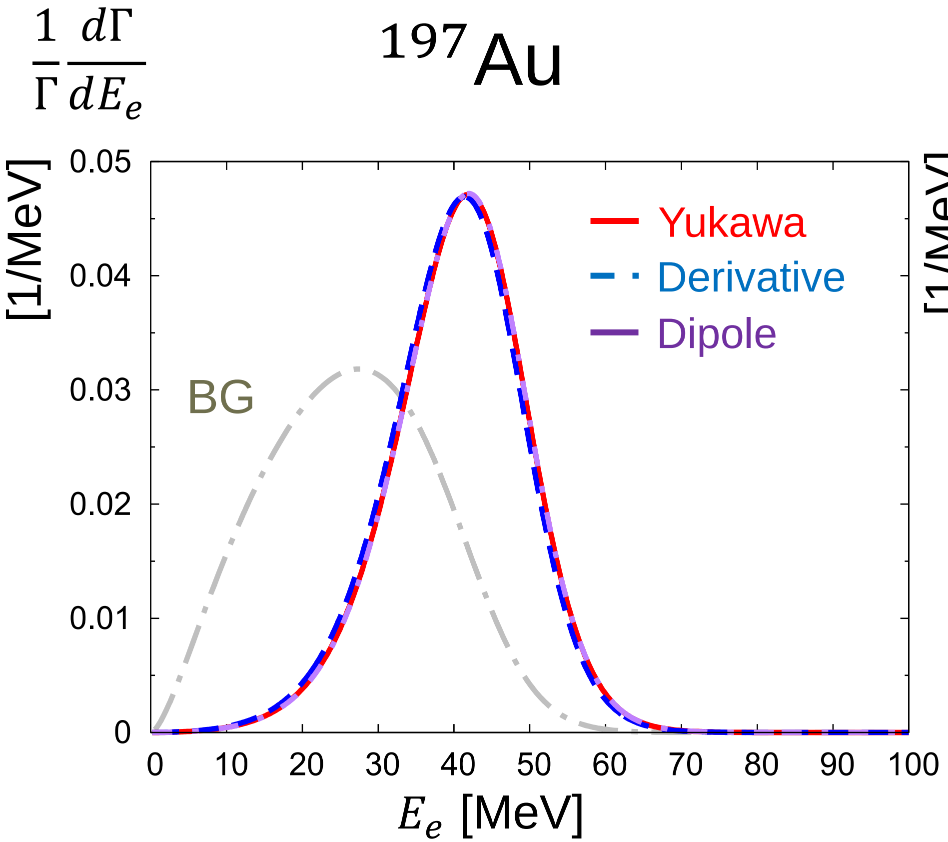

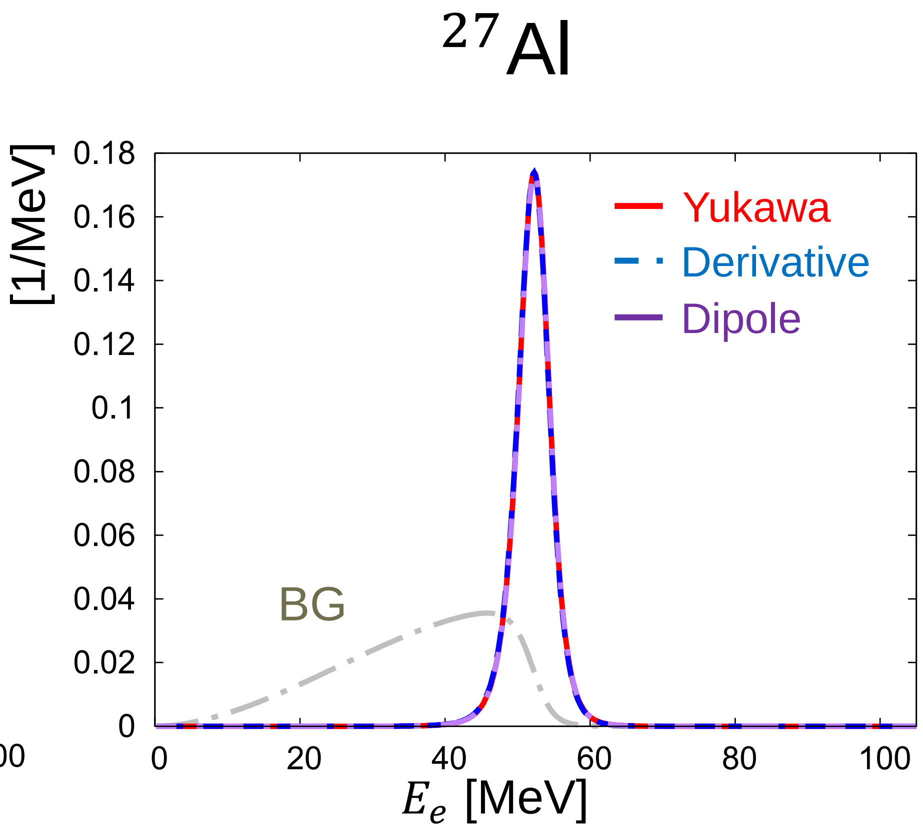

- Spectrum does not strongly depend on properties of X.
- The sharper peak is obtained for the lighter nucleus because the width reflects the shape of the bound muon w.f.

e^- spectrum near endpoint

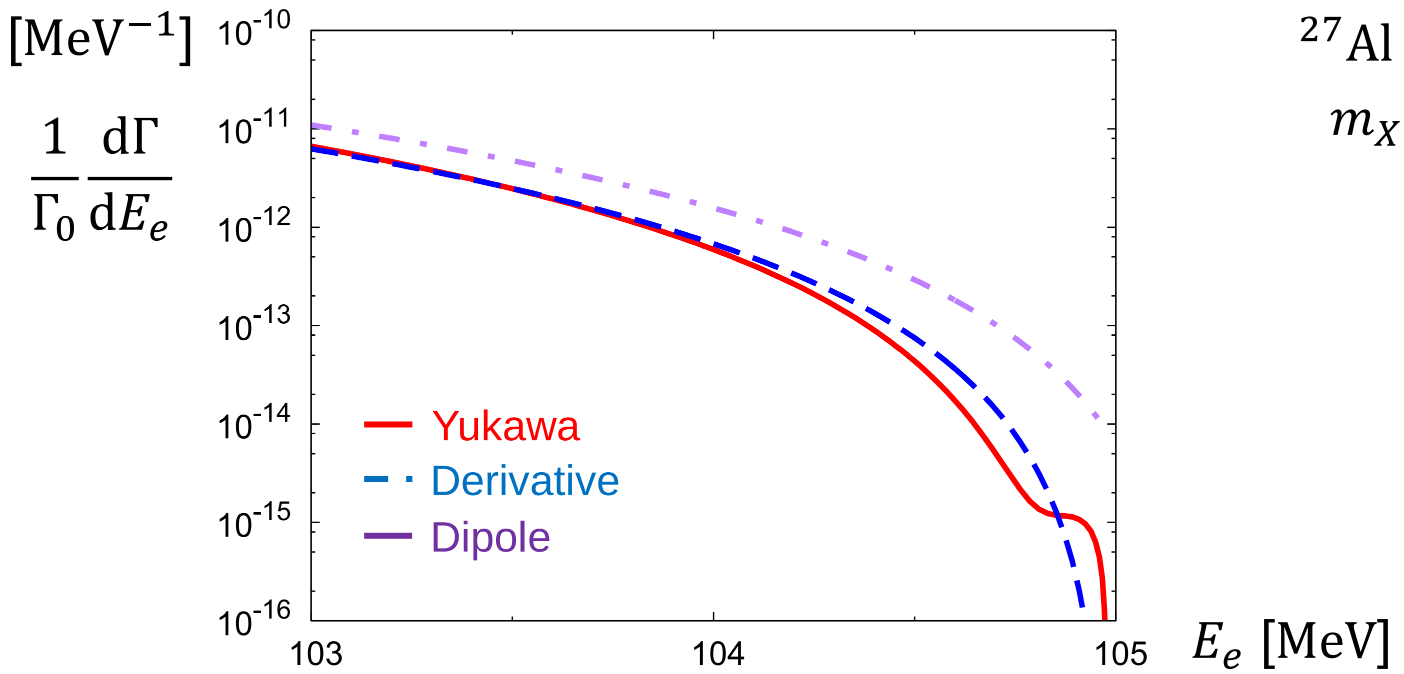

^{27}Al target

$m_X = 0$

- We can see spectra depending on operators!

Characteristic behavior of spectrum

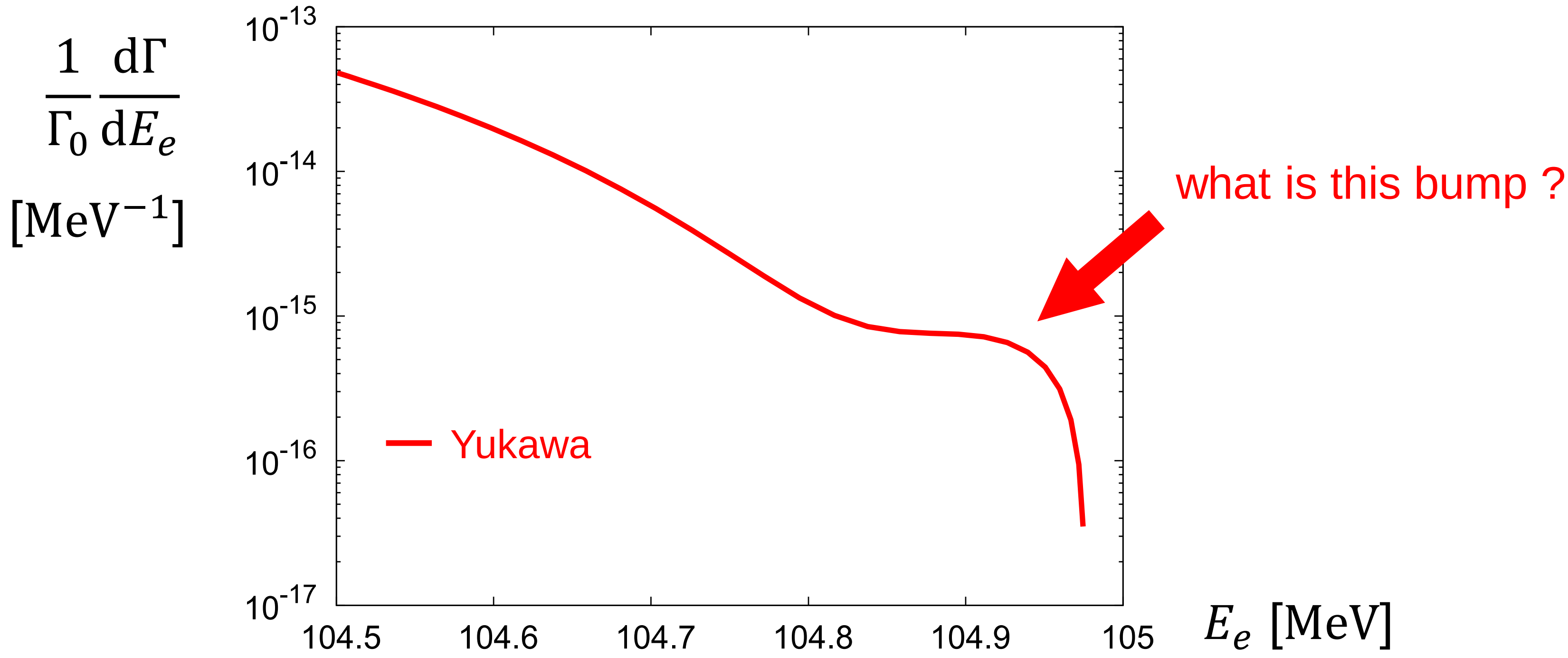

$$\frac{d\Gamma}{dE_e} = \frac{g_Y^2}{4\pi^2} p_e p_X \sum_\kappa (2j_\kappa + 1)|I_\kappa|^2$$

$$I_\kappa = \int_0^\infty dr r^2 j_{l_\kappa}(p_X r)\{g_{p_e}^\kappa(r) g_\mu^{1s}(r) - f_{p_e}^\kappa(r) f_\mu^{1s}(r)\}$$

Characteristic behavior of spectrum

✓ Main contribution comes from s-wave of emitted electron.

⇨ s-wave ($\kappa = -1$) amplitude

$$I_{-1} = m_\mu \int_0^\infty dr r^2 j_0(p_X r)\{g_{p_e}^{-1}(r) g_\mu^{1s}(r) - f_{p_e}^{-1}(r) f_\mu^{1s}(r)\}$$

$j_0(p_X r) \simeq const.$ near the endpoint

✓ $\int_0^\infty dr r^2 \{g_{p_e}^{-1}(r) g_\mu^{1s}(r) - f_{p_e}^{-1}(r) f_\mu^{1s}(r)\} = 0$ if $E_e = E_\mu = \frac{m_\mu m_N}{m_N + m_\mu} - B_{\mu N}$

reduced mass

$\int_0^\infty dr\, r^2 \{g_{p_e}^{-1}(r) g_\mu^{1s}(r) - f_{p_e}^{-1}(r) f_\mu^{1s}(r)\}$ $[\mathrm{MeV}^{-1}]$

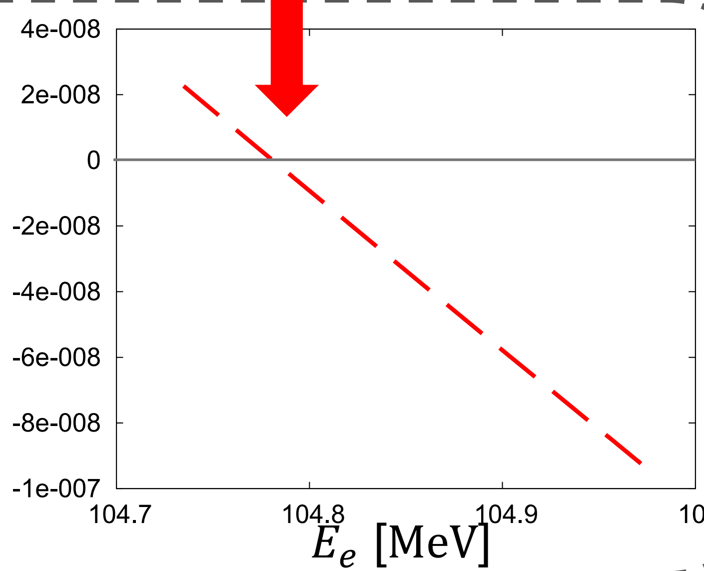

Characteristic behavior of spectrum

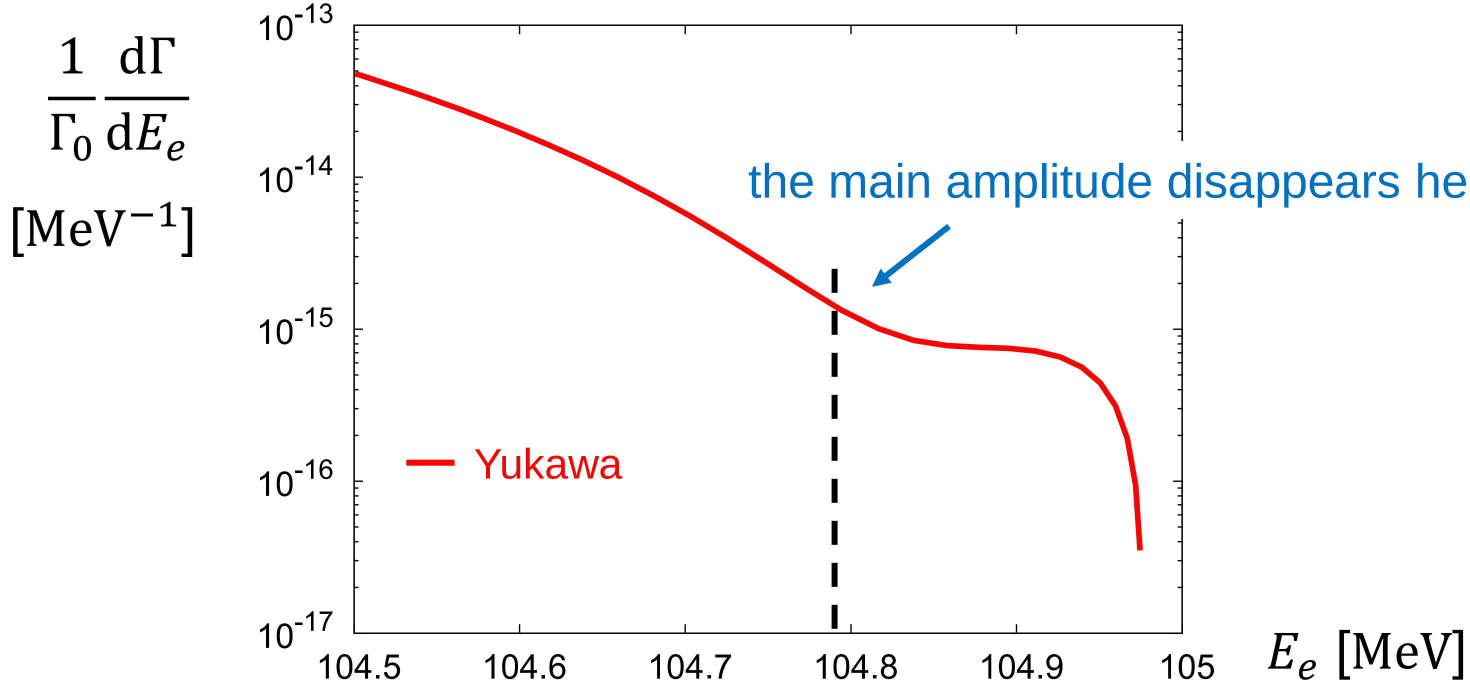

Energy to erase the main contribution :

$$\frac{m_\mu m_N}{m_N + m_\mu} - B_{\mu N} \simeq 104.79\mathrm{MeV}$$

Maximum energy of electron : $$\frac{2m_N(m_\mu - B_{\mu N}) + (m_\mu - B_{\mu N})^2}{2(m_N + m_\mu - B_{\mu N})} \simeq 104.97\mathrm{MeV}$$

Q. The reduced mass treatment is insufficient to include the nuclear mass?

5-2. $\mu^- \to e^- \gamma$

YU, M. Yamanaka, & Y. Kuno, PRD111, 035017; arXiv:2411.10304.

$\mu^- \to e^-\gamma$ in a muonic atom

◆ Rare decay of μ^- in orbit (not free μ^+)

- signal: a pair of e^- & γ with $E_e + E_\gamma = m_\mu - E_b$
  (E_b: binding energy)
- Typically, the signal e^- & γ are emitted
  back-to-back with $E_e \simeq E_\gamma \simeq 50$ MeV
  - ✓ But it's not a strict two-body decay,
    the spectrum is smeared.

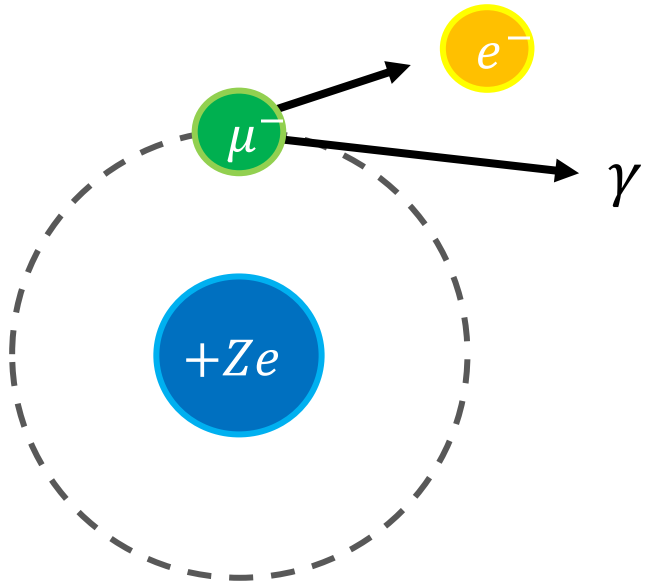

- As well as dipole operator,
  diphoton operator(FF & $F\tilde{F}$) can be studied.
  - ✓ The diphoton ope. can be directly restricted
    as $\mu^+ \to e^+\gamma\gamma$.

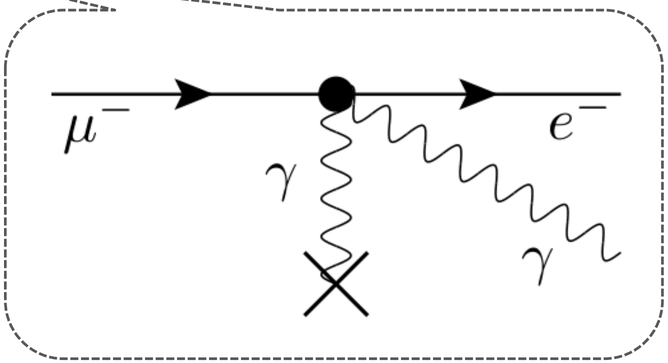

Disadvantages:

- Muonic atoms have shorter lifetime
  than free muons.
- Invariant mass $m_{e\gamma} \neq m_\mu$;
  Although the energy is (approximately) conserved, the 3-momentum is not in $\mu^- \to e^-\gamma$.

Decay rate

- Nucleus is treated as a static Coulomb potential.

$$d\Gamma = \frac{d^3p_e}{(2\pi)^3 2E_e}\frac{d^3p_\gamma}{(2\pi)^3 2E_\gamma}(2\pi)\delta\left(E_e+E_\gamma-E_\mu\right)\frac{1}{2}\sum_{spins}|\mathcal{M}|^2$$

transition amplitude

$$\begin{aligned}\mathcal{M} = &-\frac{2im_\mu}{v^2}\int d^3r\overline{\psi}_e(\boldsymbol{r})\,\sigma_{\alpha\beta}\left(D_LP_L+D_RP_R\right)\psi_\mu^{1s}(\boldsymbol{r})\,p_\gamma^\alpha\epsilon^{s_\gamma*\beta}\exp\left(-i\boldsymbol{p}_\gamma\cdot\boldsymbol{r}\right)\\ &-\frac{4i}{v^3}\int d^3r\overline{\psi}_e(\boldsymbol{r})\left(C_LP_L+C_RP_R\right)\psi_\mu^{1s}(\boldsymbol{r})\,p_\gamma^\alpha\epsilon^{s_\gamma*\beta}\exp\left(-i\boldsymbol{p}_\gamma\cdot\boldsymbol{r}\right)\langle N\,|\,F_{\alpha\beta}\,|\,N\rangle\\ &-\frac{4i}{v^3}\int d^3r\overline{\psi}_e(\boldsymbol{r})\,i\gamma_5\left(\tilde{C}_LP_L+\tilde{C}_RP_R\right)\psi_\mu^{1s}(\boldsymbol{r})\,p_\gamma^\alpha\epsilon^{s_\gamma*\beta}\exp\left(-i\boldsymbol{p}_\gamma\cdot\boldsymbol{r}\right)\left\langle N\,\middle|\,\tilde{F}_{\alpha\beta}\,\middle|\,N\right\rangle\end{aligned}$$

→ The field strength F is replaced with nuclear electric field E.

$$\langle N\,|\,F_{\alpha\beta}\,|\,N\rangle = \begin{cases}-E_i & (\alpha=i,\beta=0)\\ E_j & (\alpha=0,\beta=j)\\ 0 & (\alpha=i,\beta=j)\end{cases} \qquad \left\langle N\,\middle|\,\tilde{F}_{\alpha\beta}\,\middle|\,N\right\rangle = \begin{cases}-\epsilon_{ijk}E_k & (\alpha=i,\beta=j)\\ 0 & (\alpha=0 \text{ or } \beta=0)\end{cases}$$

※ In this calculation, we restrict ourselves to the case that the proton number is small.

→ We assume “The nucleus is point-charge.” & “The electron is plane wave.”

Z dep. of the decay rate ($Z \leq 30$)

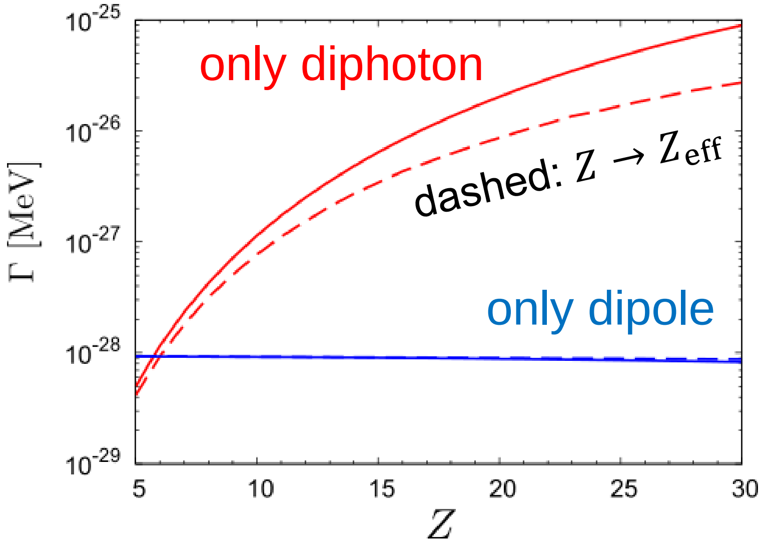

$\Gamma_{FF} \propto Z^5$

$Z^3 \leftarrow$ muon w.f.

$Z^2 \leftarrow (E)^2$

$\Gamma_D \propto 1$

(moderately decreasing)

- Upper limits of BR from the past experiments

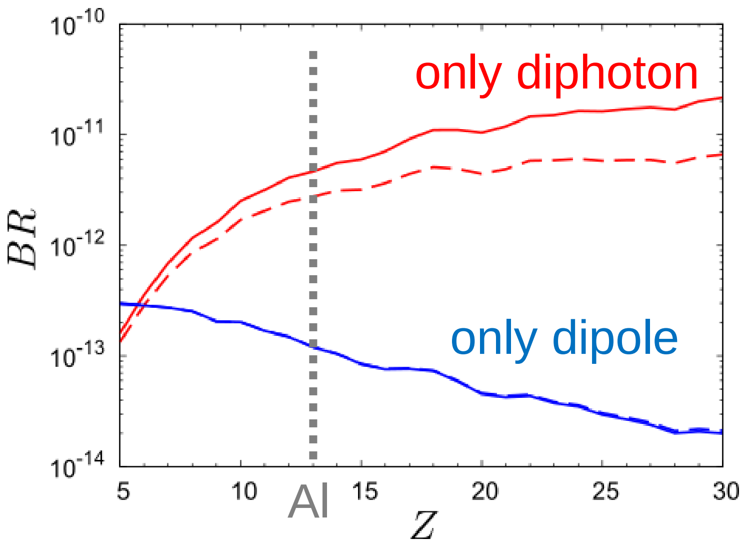

$BR(\mu^+ \to e^+\gamma\gamma) < 7.2 \times 10^{-11}$

$BR < 4.6 \times 10^{-12}$ for Al

$BR(\mu^+ \to e^+\gamma) < 3.1 \times 10^{-13}$

$BR < 1.2 \times 10^{-13}$ for Al

Energy & angular distribution

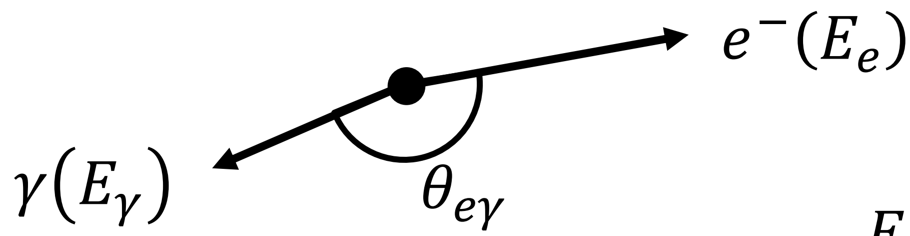

$$E_\mu = E_e + E_\gamma$$

- energy distribution Al ($Z = 13$)

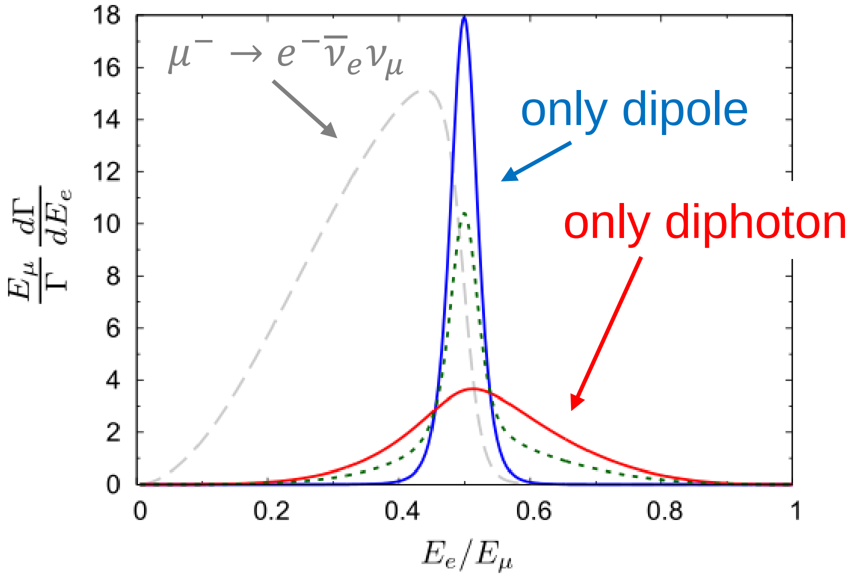

- angular distribution Al ($Z = 13$)

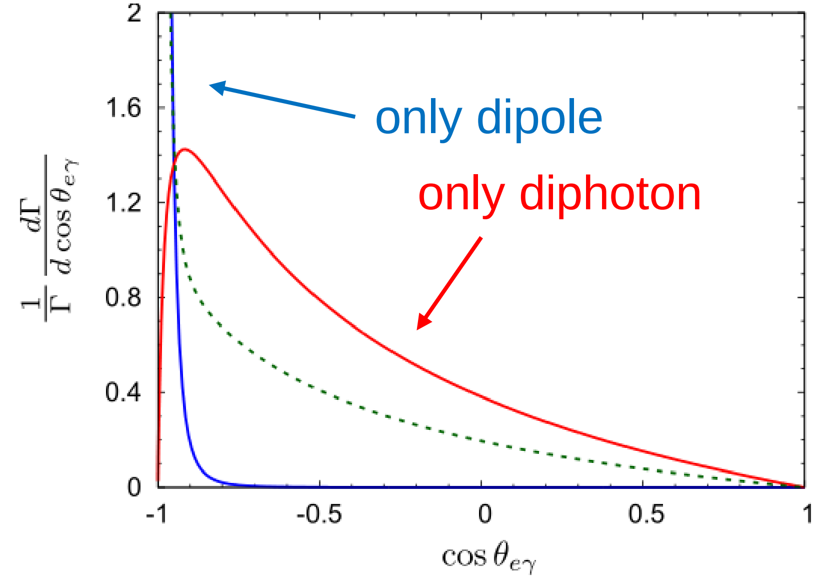

(green dashed: case that dipole & diphoton are equally interfered)

✓ diphoton : momentum distribution spreads more than dipole

(dipole & diphoton are interfered, but 分布の形状が異なる=完全に打ち消されることはない)

Backgrounds

✓ Electrons & photons are produced in the ordinary muon decays:

1. $\mu^- \to e^- \nu_\mu \overline{\nu}_e$

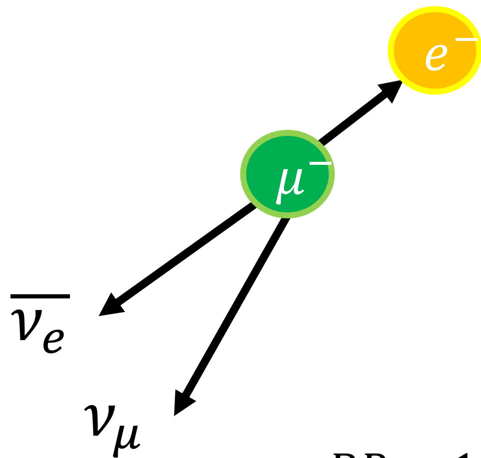

$BR \sim 1$

2. $\mu^- \to e^- \nu_\mu \overline{\nu}_e \gamma$

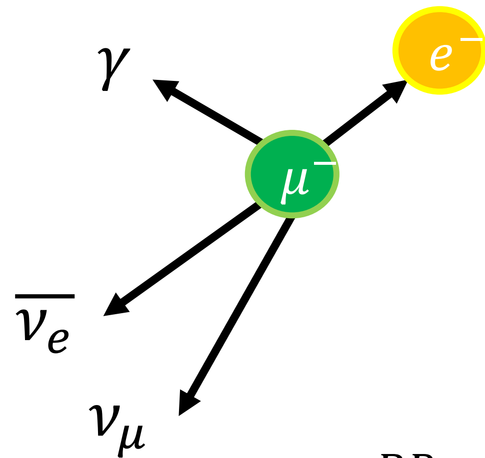

$BR \sim 10^{-7}$

➢ BG1: 2つのミューオンから出た電子と光子のエネルギー和が信号のものと偶然一致する事象 (accidental BG)

$E_e + E_\gamma = m_\mu - E_b$

➢ BG2: $\mu^- \to e^- \nu_\mu \overline{\nu}_e \gamma$ におけるニュートリノが低エネルギーである事象 (physics BG)

(ただし これは無視できるほど小さい)

BG e^- & γ spectra

E_e distribution

$\mu^- \to e^- \nu_\mu \bar{\nu}_e$

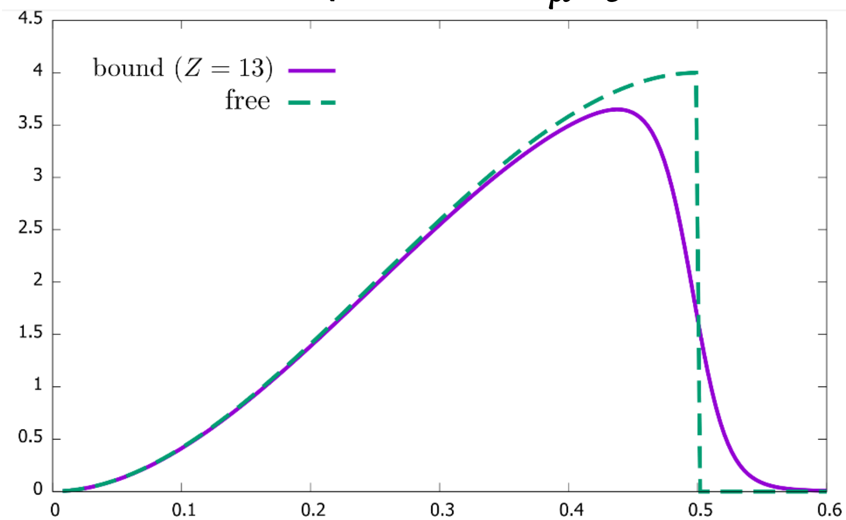

E_e/m_μ

E_γ distribution

$\mu^- \to e^- \nu_\mu \bar{\nu}_e \gamma$

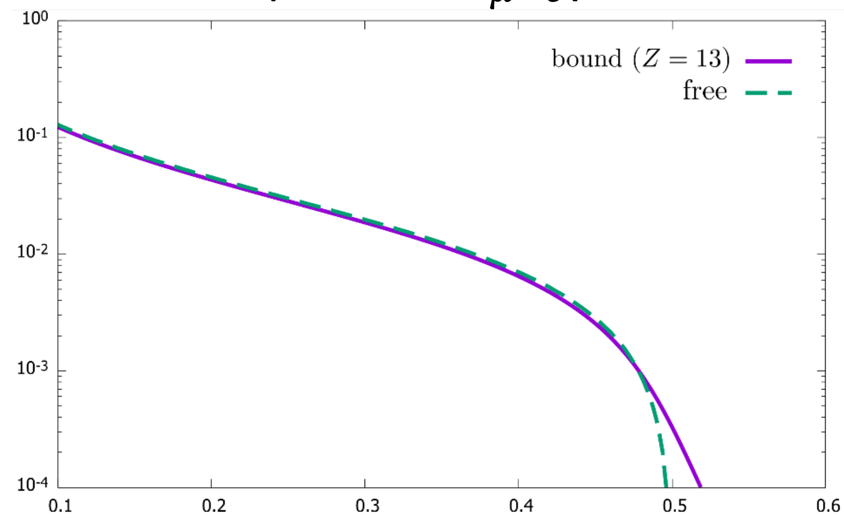

E_γ/m_μ

The value at $E_\gamma = m_\mu/2$ is 0 in free muon, but it is nonzero in bound muon…

Effective branching ratio

Benchmark : energy resolution

$R_\mu = 10^7$ /s $\Delta t_{e\gamma} = 78$ ps $\Delta_{x+y} = 0.01$

Effective BR

$$B_{acc} = R_\mu \Delta t_{e\gamma} \frac{\Delta\Omega_{e\gamma}}{4\pi} f_{acc}$$

R_μ: produced μ^-/ time

$\Delta t_{e\gamma}$: time resolution

$\Delta\Omega_{e\gamma}$: angular resolution

f_{acc}: the rate that BG e^- & γ satisfy the energy condition

	Al ($Z = 13$)	Zn ($Z = 30$)
Signal (diphoton)	4.6×10^{-12}	2.2×10^{-11}
Signal (dipole)	1.2×10^{-13}	2.0×10^{-14}
accidental BG	1.2×10^{-10}	1.2×10^{-11}
BG ($\mu^- \to e^-\nu\bar{\nu}\gamma$)	1.5×10^{-15}	5.7×10^{-16}

(negligible)

large BGs…

constraint $\theta_{e\gamma}$ to optimize diphoton signal

$$\theta_{e\gamma}^{peak} - 0.01 < \theta_{e\gamma} < \theta_{e\gamma}^{peak} + 0.01$$

$\theta_{e\gamma}^{peak} = 2.39$ for Al

$\theta_{e\gamma}^{peak} = 2.13$ for Zn

	Al ($Z = 13$)	Zn ($Z = 30$)
Signal (diphoton)	7.1×10^{-14}	3.3×10^{-13}
Signal (dipole)	1.2×10^{-17}	1.6×10^{-17}
accidental BG	8.5×10^{-13}	1.1×10^{-13}
BG ($\mu^- \to e^-\nu\bar{\nu}\gamma$)	2.6×10^{-19}	6.1×10^{-19}

Signal is twice larger than BG !

↑ There may be rooms for further optimization.

5-3. $\mu^- e^- \to e^- e^-$

YU, Y. Kuno, J. Sato, T. Sato, & M. Yamanaka, PRD93, 076006; arXiv:1603.01522.

YU, Y. Kuno, J. Sato, T. Sato, & M. Yamanaka, PRD97, 015017; arXiv:1711.08979.

$\mu^- e^- \to e^- e^-$ in a muonic atom

M. Koike, Y. Kuno, J. Sato & M. Yamanaka,
Phys. Rev. Lett. **105**, 121601 (2010).

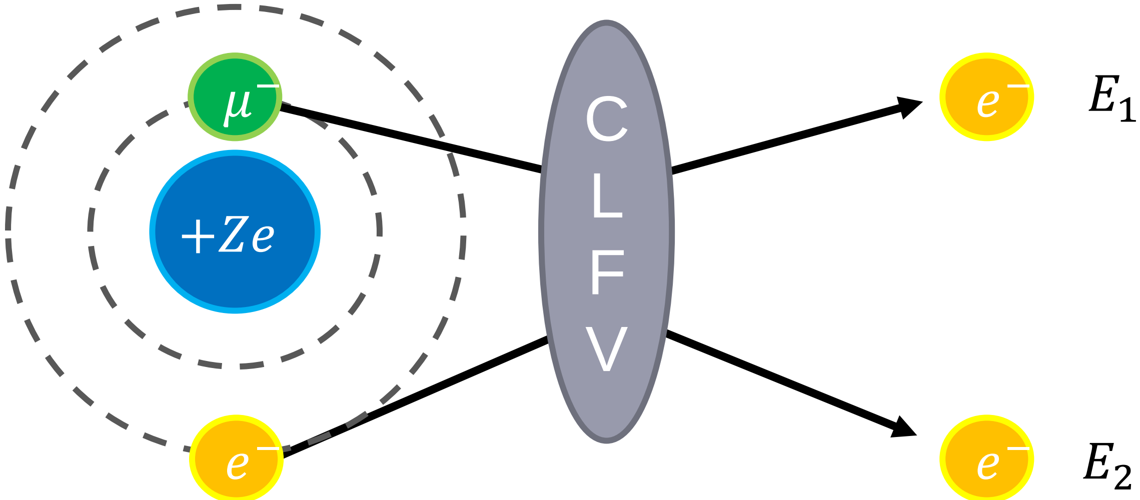

- clear signal : $E_1 + E_2 \simeq m_\mu + m_e - B_\mu - B_e$
- 2 CLFV mechanisms
  - ✓ contact (μeee vertex)
  - ✓ photonic ($\mu e\gamma$ vertex)

  (similar to $\mu^+ \to e^+ e^+ e^-$)

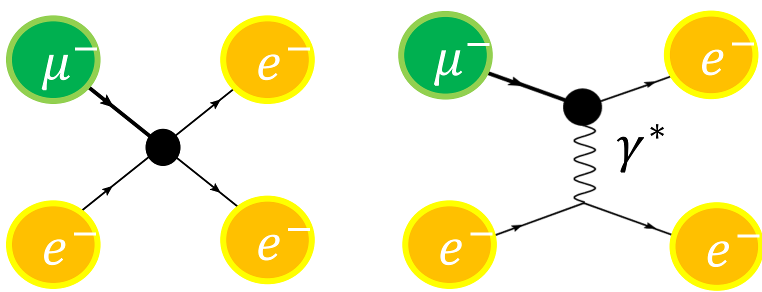

- atomic # Z : large ⇒ decay rate Γ : large $\left(\Gamma \propto (Z-1)^3\right)$

Effective Lagrangian for $\mu^- e^- \to e^- e^-$

$$\mathcal{L}_I = \mathcal{L}_{contact} + \mathcal{L}_{\mu\to e\gamma}$$

$$\mathcal{L}_{\text{contact}} = -\frac{4G_F}{\sqrt{2}}\left[g_1(\overline{e_L}\mu_R)(\overline{e_L}e_R) + g_2(\overline{e_R}\mu_L)(\overline{e_R}e_L) + g_3(\overline{e_R}\gamma_\mu\mu_R)(\overline{e_R}\gamma^\mu e_R) + g_4(\overline{e_L}\gamma_\mu\mu_L)(\overline{e_L}\gamma^\mu e_L) + g_5(\overline{e_R}\gamma_\mu\mu_R)(\overline{e_L}\gamma^\mu e_L) + g_6(\overline{e_L}\gamma_\mu\mu_L)(\overline{e_R}\gamma^\mu e_R)\right] + [H.c.]$$

$$\mathcal{L}_{\mu\to e\gamma} = -\frac{4G_F}{\sqrt{2}} m_\mu\left[A_R\overline{e_L}\sigma^{\mu\nu}\mu_R F_{\mu\nu} + A_L\overline{e_R}\sigma^{\mu\nu}\mu_L F_{\mu\nu}\right] + [H.c.]$$

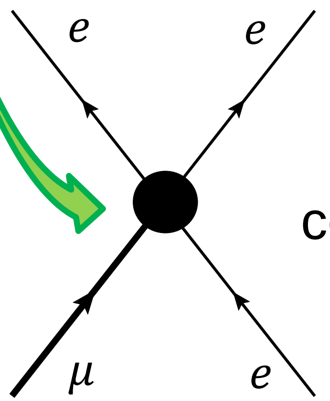

contact interaction

constrained by $\mu \to eee$

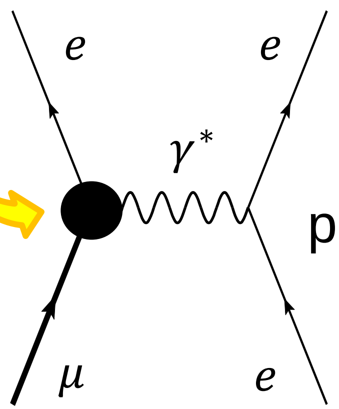

photonic interaction

constrained by $\mu \to e\gamma$

Compared to $\mu^+ \to e^+ e^- e^+$

$\mu^- e^- \to e^- e^-$ in muonic atoms

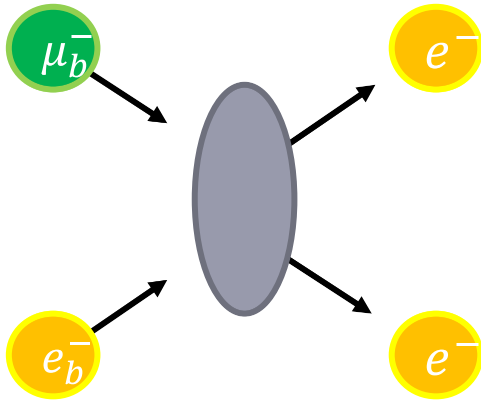

$\mu^+ \to e^+ e^- e^+$

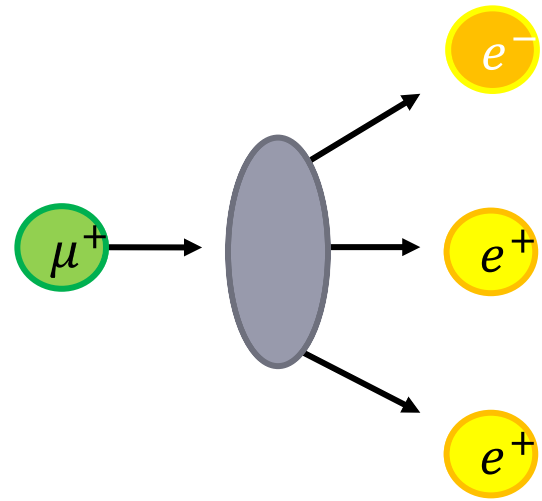

Difference 1 : signals

two e^-

(approximately) 2-body decay

one e^- & two e^+

3-body decay

Difference 2 : interference between LFV operators

e.g., Do $(\overline{e}_R \mu_L)(\overline{e}_R e_L)$ & $(\overline{e}_R \gamma_\mu \mu_R)(\overline{e}_R \gamma^\mu e_R)$ interfere?

Yes

No

Branching ratio

How many muonic atoms decay with CLFV, compared to created # ?

$$\mathrm{BR}(\mu^- e^- \to e^- e^-) \equiv \tilde{\tau}_\mu \Gamma(\mu^- e^- \to e^- e^-)$$

$\Gamma \propto (Z-1)^3$
due to existence prob. of bound e^- at the origin

$\tilde{\tau}_\mu$: lifetime of a muonic atom

cf. $2.2\mu\mathrm{s}$ for a muonic H ($Z = 1$)
$80\mathrm{ns}$ for a muonic Pb ($Z = 82$)

BR with CLFV coupling fixed on allowed maximum

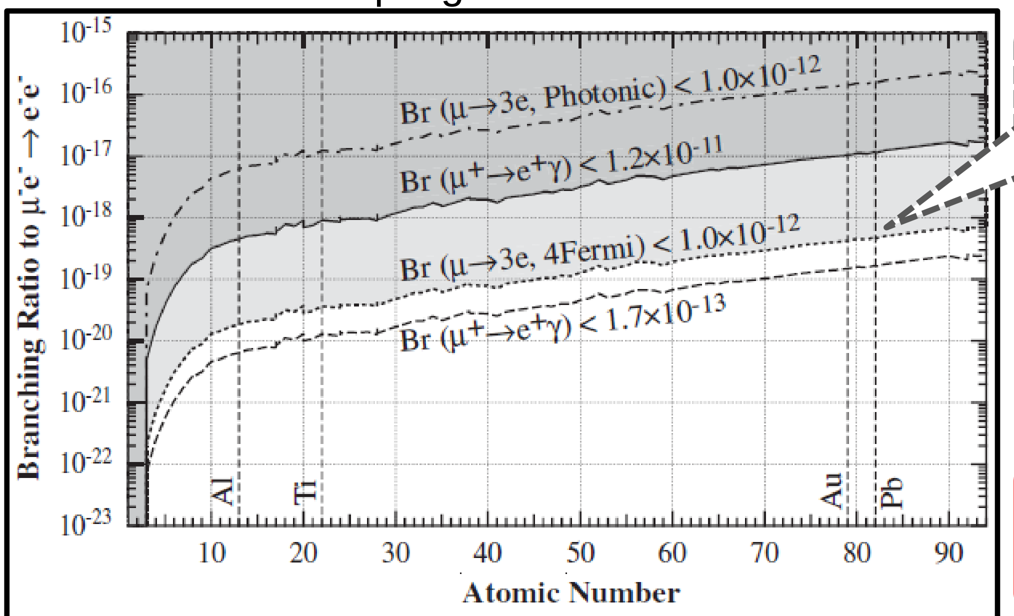

Phys. Rev. Lett. **105**,121601 (2010).

e.g. $\mathrm{BR} < 5.0 \times 10^{-19}$ for Pb ($Z = 82$)
if contact process is dominant

➢ BR increases with atomic # Z.

⇩

Using muonic atoms with large Z is favored to search for $\mu^- e^- \to e^- e^-$.

To improve calculation for decay rate

✓ previous formula of CLFV decay rate by Koike *et al.*

$$\Gamma_{\mu^- e^- \to e^- e^-} = 2\sigma v_{\mathrm{rel}} |\psi_{1S}^e(0)|^2 \propto (Z-1)^3$$

Note

- ➢ "Z dependence" comes from only $|\psi_{1S}^e(0)|^2$ (always $\Gamma \propto (Z-1)^3$)
- ➢ emitted e^-s are expected to be back-to-back with equal energies

used approximations ($Z\alpha \ll 1$)

- spatial extension of bound lepton $\gg$ wave length of emitted e^-
- bound lepton : non-relativistic
- emitted e^- : plane wave

In atoms with large Z,

- ← *small orbital radius*
- ← *relativistic (especially, e^-)*
- ← *Coulomb distortion*

More quantitative estimation is needed ! (important for large Z)

Formulation for decay rate

$$\Gamma = \sum_f \sum_{\bar{i}} (2\pi)\delta(E_f - E_i) \left| \left\langle \psi_e^{\boldsymbol{p}_1,s_1} \psi_e^{\boldsymbol{p}_2,s_2} \middle| H \middle| \psi_\mu^{1s,s_\mu} \psi_e^{1s,s_e} \right\rangle \right|^2$$

partial wave expansion to express the distortion

$$\psi_e^{\boldsymbol{p},s} = \sum_{\kappa,\mu,m} 4\pi\, i^{l_\kappa} (l_\kappa, m, 1/2, s | j_\kappa, \mu) Y^*_{l_\kappa,m}(\hat{p}) e^{-i\delta_\kappa} \psi_p^{\kappa,\mu}$$

κ : index of angular momentum

solving “Dirac eq. with ϕ” numerically to get radial wave functions

$$\frac{dg_\kappa(r)}{dr} + \frac{1+\kappa}{r} g_\kappa(r) - \big(E + m + e\phi(r)\big) f_\kappa(r) = 0$$

$$\frac{df_\kappa(r)}{dr} + \frac{1-\kappa}{r} f_\kappa(r) + \big(E - m + e\phi(r)\big) g_\kappa(r) = 0$$

ϕ : nuclear Coulomb potential

$$\psi(\boldsymbol{r}) = \begin{pmatrix} g_\kappa(r)\chi_\kappa^\mu(\hat{r}) \\ i f_\kappa(r)\chi_{-\kappa}^\mu(\hat{r}) \end{pmatrix}$$

Upper limits of BR (contact process)

$BR(\mu^+ \to e^+e^-e^+) < 1.0 \times 10^{-12}$ → $BR(\mu^-e^- \to e^-e^-) < B_{max}$

(SINDRUM, 1988)

$(g_1(\overline{e_L}\mu_R)(\overline{e_L}e_R))$

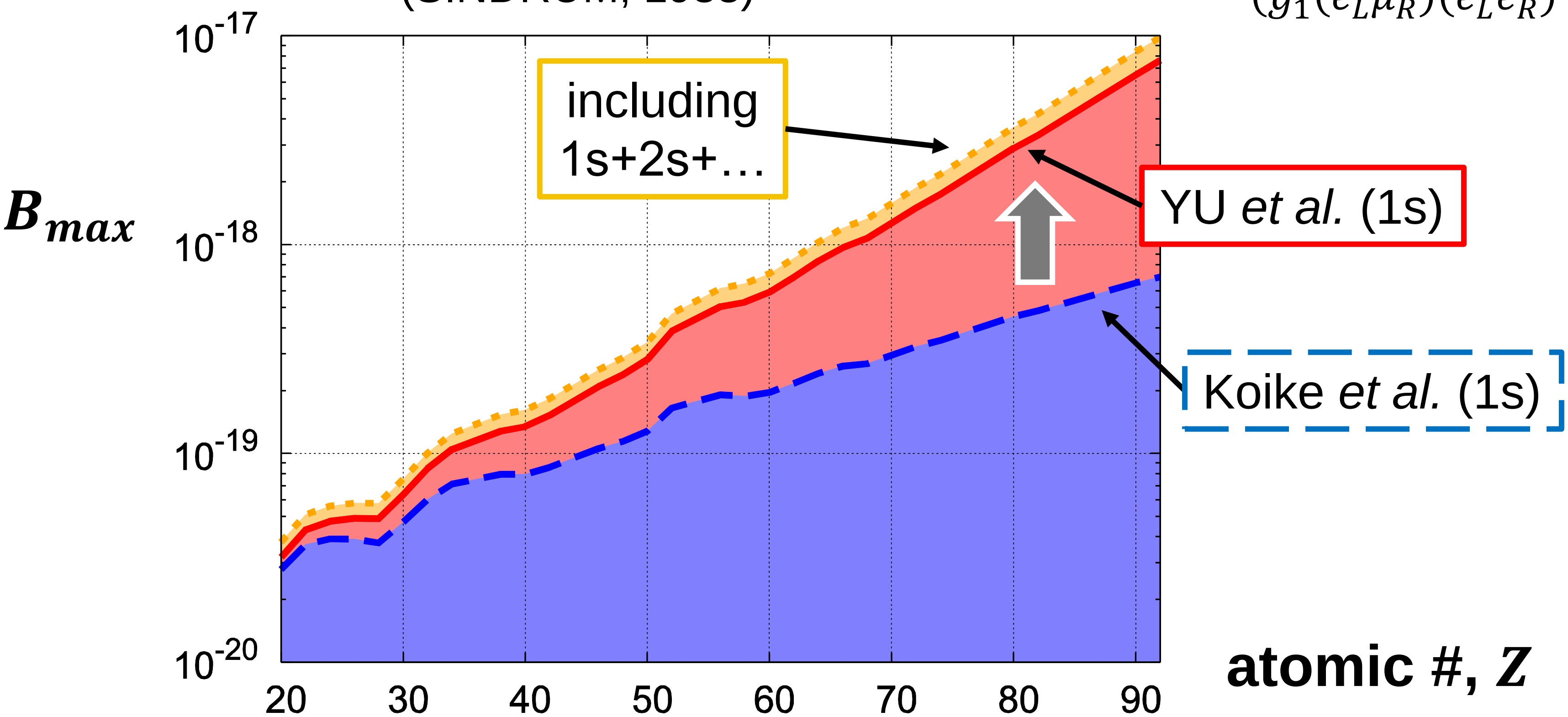

YU, Y. Kuno, J. Sato, T. Sato & M. Yamanaka, Phys. Rev. D **93**, 076006 (2016).

inverse of B_{max} $(Z = 82)$

2.1×10^{18} → 3.0×10^{17}

Upper limits of BR (photonic process)

$BR(\mu^+ \to e^+\gamma) < 4.2 \times 10^{-13}$ → $BR(\mu^- e^- \to e^- e^-) < B_{max}$

(MEG, 2016)

$(A_R \overline{e_L} \sigma^{\mu\nu} \mu_R F_{\mu\nu})$

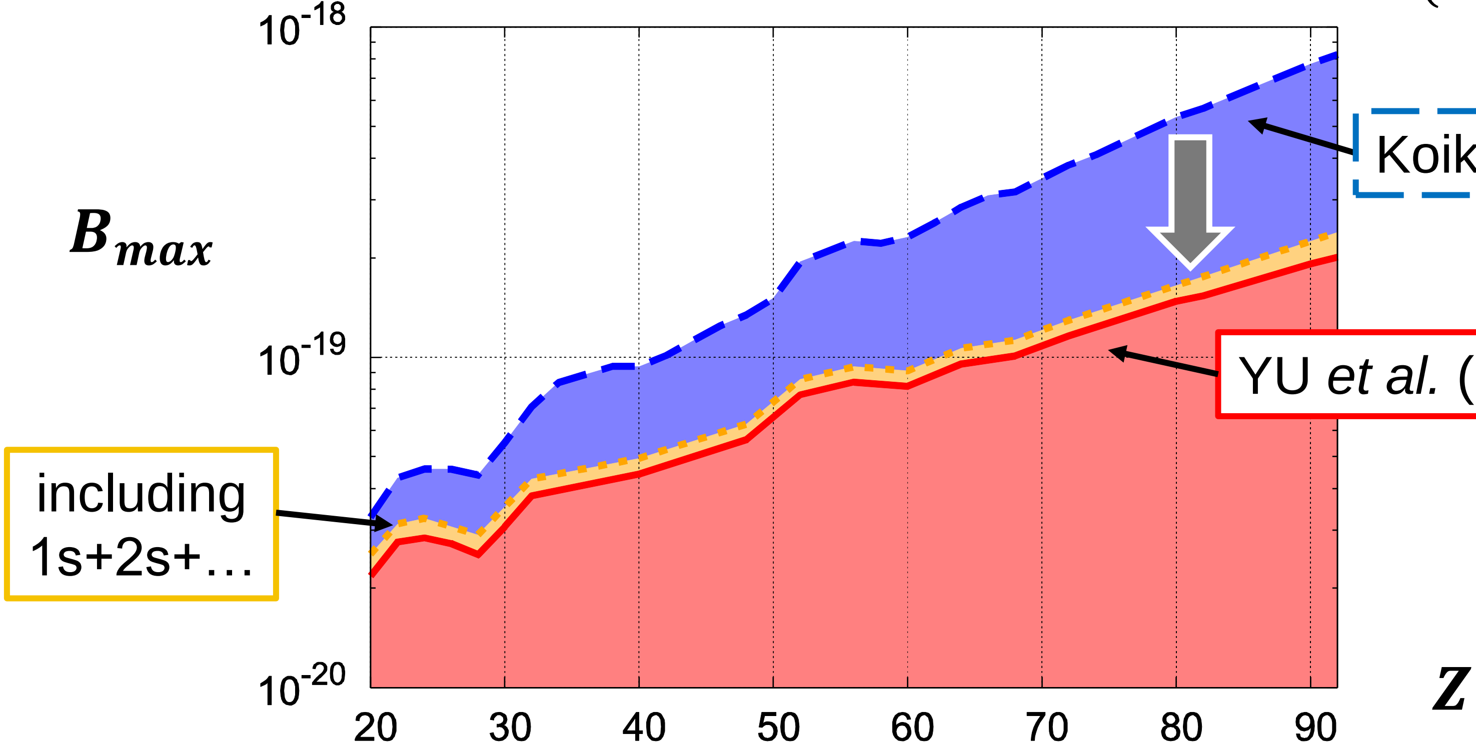

YU, Y. Kuno, J. Sato, T. Sato & M. Yamanaka, Phys. Rev. D **97**, 015017 (2018).

inverse of B_{max} $(Z = 82)$

1.8×10^{18} → 6.6×10^{18}

6. Summary

Summary

- For quantitively calculating muon decays in nuclei, we need to solve the Dirac equation with the nuclear Coulomb field, for μ^- & e^-.

- Some LFV processes on nuclei are discussed:
  - DIO, $\mu^- \to e^- \nu_\mu \overline{\nu}_e$
  - $\mu^- \to e^-$ conversion
  - Other possible LFVs
    - $\mu^- \to e^- X$
    - $\mu^- \to e^- \gamma$
    - $\mu^- e^- \to e^- e^-$